Density and Viscosity for the Non-aqueous and Aqueous Mixtures of Methyldiethanolamine and Monoethylene Glycol at Temperatures from 283.15 K to 353.15 K

*Eirini Skylogianni, Ricardo R. Wanderley, Sigrid S. Austad, Hanna K. Knuutila**

Department of Chemical Engineering, Norwegian University of Science and Technology, 7034 Trondheim, Norway

ABSTRACT

Non-aqueous and aqueous mixtures of methyldiethanolamine and monoethylene glycol form promising absorbents for the combined hydrogen sulfide removal and hydrate control, necessary in natural gas processing. In this direction, the density and viscosity of the binary and ternary systems were measured and modeled in the temperature range of T = (283.15 to 353.15) K and ambient pressure. Excess molar volumes and viscosity deviations from ideality were also calculated. The water content varied from 5 to 50 wt.% and the amine content from 5 to 90 wt.%. Both density and viscosity were modeled using non-random two liquid NRTL-based models. Regarding the density modeling, the average absolute relative deviations (AARD) were found to be less than 0.5% for the binary subsystems and equal to 0.2% for the ternary system. Viscosity modeling results show higher AARD, though always lower than 3.0% for both binary and ternary solutions.

1. INTRODUCTION

Acid gas removal with the aid of amines is a common industrial process, for example in oil refineries and natural gas treatment plants among others. Commercial amines are monoethanolamine (MEA), diglycolamine (DGA) and methyldiethanolamine (MDEA), the latter being most suitable for the selective removal of hydrogen sulfide (H_2S) over carbon dioxide (CO_2)[1]. In oil and gas production, hydrate control or dehydration is an equally necessary process as gas sweetening. Typically, glycols such as monoethylene glycol (MEG) and triethylene glycol (TEG) are used respectively to prevent hydrate formation during gas transportation and to reach water content specifications[2,3]. Moreover, the focus of oil and gas companies on subsea operations encourages process intensification concepts, where modules with respect to size, weight and complexity are developed[4]. Such concept is the combined removal of acid gases and water vapors in one-step only, firstly conceived and patented by Hutchinson[5] and later further developed by McCartney[6,7] and Chapin[8]. In this direction, our group investigates the feasibility of simultaneous acid gas removal and hydrate control process with non-aqueous and aqueous MDEA-MEG mixtures.

As in every new process analysis, the evaluation of the combined acid gas and water vapor removal by an amine-glycol based solvent requires the knowledge of the thermodynamic behavior, reaction kinetics and physical properties of the system. This study focuses on some of the physical properties of the system, namely density and viscosity, which play a crucial role for the successful design and operation of a separation process. Nookueaa et al. studied the effect of various thermo-physical properties on the design of an absorber for CO_2 capture and concluded that liquid density and viscosity have the most significant impact on the packing height[9]. Especially for subsea application, the low temperature experienced in the seabed dramatically changes the solvent's viscosity, affecting the overall mass transfer and hydrodynamics of the system. In fact, viscosity specifications related to

pumpability of injected chemicals apply for offshore/subsea operations. Therefore, the objective of this study is to provide experimental measurements and develop auxiliary models for density and viscosity as a tool for assessing the successful employment of the binary MDEA-MEG or the ternary MDEA-MEG-H_2O systems for natural gas purification.

The literature is rich in density and viscosity studies for aqueous MDEA solutions, due to its broad applicability in CO_2 capture and selective H_2S removal. Several authors report densities[10–14] and viscosities[11–19] of MDEA-H_2O mixtures. Moreover, measuring density and viscosity of pure MDEA has been presented as validation for the experimental method of density and viscosity measurements[20]. Sufficient amount of data exist also for MEG-H_2O system densities and viscosities[21–26]. A comprehensive, though not exhaustive, list is shown in **Table 1**. The combination of amines and glycols has also been studied in the literature[27–30], however, to our best knowledge, no data on the density or the viscosity of the MDEA-MEG or MDEA-MEG-H_2O mixtures are reported. In addition, although for pure monoethylene glycol and its solutions with water, density and viscosity measurements have been reported at low temperatures, even down to 263 K [22,24,26], only Bernal-Garcia et al.[10] report densities at 283.15 K for pure MDEA and its aqueous solutions. We have not found reported viscosities of pure MDEA or aqueous MDEA in the existing literature at such low temperature.

In this work, density and viscosity measurements of the binary system MDEA-MEG and the ternary system MDEA-MEG-H_2O are presented in the temperature range of T = (283.15 to 353.15) K and pressure of 0.1020 MPa. The binary system was studied in the whole concentration range, from pure MDEA to pure MEG. For the ternary system of aqueous MDEA-MEG, we varied the water concentration from 5 wt.% to 50 wt.% in order to demonstrate the impact of water content in the physical properties of the amine-glycol system studied. Both density and viscosity were modeled for

67 the pure components, binary and ternary systems using the data obtained in this work as well as the
68 data presented in **Table 1**.

69 **Table 1:** Literature Review on the Density and Viscosity Measurements for Aqueous MDEA and
70 Aqueous MEG Systems at Ambient Pressure

System	Molar Fraction, x_1	Property	Temperature (K)	Source
MDEA (1)	0 - 1	Density	283.15 - 363.15	Bernal-Garcia et al.[10]
H_2O (2)	0.0165 - 1	Density	288.15 - 333.15	Al-Ghawas et al.[11]
	0.0165 - 1	Viscosity	288.15 - 333.15	
	0.0364, 0.0608	Density	303.15 - 333.15	Li and Lie[12]
	0.0364 - 1	Viscosity	303.15 - 353.15	
	0.0165 - 1	Density	288.15 - 333.15	Paul and Mandal[13]
	0.0165 - 1	Viscosity	288.15 - 333.15	
	0.1 - 1	Density	293.15 - 333.15	Yin et al.[14]
	0.1 - 1	Viscosity	293.15 - 333.15	
	0 - 1	Viscosity	298.15 - 353.15	Teng et al.[15]
	0 - 1	Viscosity	313.15 - 363.15	Bernal-Garcia et al.[16]
	0 - 1	Viscosity	303.15 - 323.15	Chowdhury et al.[18]
	0.0447 - 1	Viscosity	293.15 - 353.15	Pinto et al.[17]
	0.0165 - 0.1313	Viscosity	333.15 - 373.15	Rinker et al.[19]
	1	Density	296.15 - 470.15	DiGuillo et al.[31]
	1	Viscosity	293.15 - 424.15	
	1	Density	298.15 - 323.15	Alvarez et al.[32]
	1	Viscosity	298.15 - 323.15	
	1	Viscosity	298.15 - 343.15	Henni et al. [33]
	1	Viscosity	303.15 - 343.15	Baek et al.[20]
	1	Viscosity	303.15 - 353.15	Haghtalab and Shojaeian[34]
	1	Viscosity	303.15 - 313.15	Akbar and Murugesan[35]
MEG (1)	0 - 1	Density	298.15	Hayduk and Malik[21]
H_2O (2)	0 - 1	Viscosity	298.15	
	0 - 1	Density	263.15 - 423.15	Bohne et al.[22]
	0 - 1	Viscosity	263.15 - 373.15	
	0.25 - 0.75	Density	296.15 - 445.15	Sun and Teja[23]
	0 - 1	Viscosity	284.15 - 449.15	
	0 - 1	Density	273.15 - 363.15	Afzal et al.[26]
	0 - 0.72	Density	293.15	Tsierkezos and Molinou[36]
	0 - 0.72	Viscosity	293.15	
	0 - 1	Density	293.15 - 353.15	Yang et al.[24]
	0 - 1	Viscosity	293.15 - 353.15	
	0 - 1	Density	283.15 - 313.15	Tsierkezos and Molinou[25]
	0 - 1	Viscosity	283.15 - 313.15	
	0 - 1	Viscosity	298.15	Jerome et al.[37]

0 - 1	Viscosity	298.15	Dunstan[38]	
1	Viscosity	298.15 - 373.15	Rumble[39]	

2. EXPERIMENTAL AND COMPUTATIONAL METHODS

2.1. Materials

Information for the chemicals used are provided in **Table 2**. The chemicals were used as received from the supplier without further purification. For the aqueous mixtures composed of MDEA-MEG-H_2O, deionized water was used. The solutions were prepared gravimetrically in a METTLER PM1200 scale with an accuracy of $1 \cdot 10^{-6}$ kg and MDEA concentration was verified for each system by acid-base titration. Magnetic stirring prior to measurements for at least 8 hours ensured solution homogeneity.

Table 2: Chemical Sample Table

Component	UIPAC name	CAS	Supplier	Mass fraction
N-methyldiethanolamine (MDEA)	2-[2-hydroxyethyl(methyl) amino] ethanol)	105-59-9	Sigma-Aldrich	≥ 0.99
monoethylene glycol (MEG)	ethane-1,2-diol	107-21-1	Sigma-Aldrich	0.998

2.2. Experimental methods

Density measurements: The densities of all solutions were measured with an Anton Paar Density Meter DMA 4500M. Millipore water and dry air were used for calibration of this apparatus, as explained by Hartono et al.[40], while pure water, MDEA and MEG were used as reference fluids for the apparatus validation. We studied the repeatability of the density measurements (Set A) at selected

temperatures at low and high concentration of MDEA-MEG, as well as at 353.15 K for the aqueous system due to the risk of water vaporization. A reproducibility study (Set C) was also performed by preparing fresh solutions and experimentally determining the density of the pure components and the binary system at low and high concentration. The results show excellent repeatability and reproducibility with average absolute relative deviations equal to 0.01% and 0.02% respectively.

Viscosity measurements: Viscosity measurements were performed in a Lovis 2000 M microviscometer, connected in series to the density meter. The sample is introduced to a temperature-controlled capillary block with an accuracy of 0.02 K, where the Hoeppler's falling ball method is employed. In our experiments, a capillary of a $1.59 \cdot 10^{-3}$ m diameter with a gold ball was used, allowing for the measurement of viscosities up to approximately 60 mPa·s. The apparatus validation presented in the section *3. Results and Discussion* revealed an AARD from reference liquids value of 2.88%. The repeatability (Set A) and reproducibility (Set C) of the viscosity measurements were studied similarly to density measurements and the AARDs are 0.76% and 0.69% respectively.

An Xsample 452 H sample filling module is integrated to the density meter and microviscometer for automatic sampling, cleaning and drying. The measurements always started with an air check and measurement of Millipore water samples, which were distributed in approximately every other three samples allowing for a continuous check of the results as well as an additional cleaning media.

For viscosities outside the limits of the available capillary in the microviscometer, an Anton Paar MCR 100 rheometer with a double gap measuring cell (DG-26.7) was used. A detailed description of the apparatus, experimental and calibration procedure is given by Hartono et al.[40] The measurements' repeatability was studied for all systems at 283.15 K and we concluded that the repeatability of the instrument is good since the maximum absolute relative deviation (MARD) is 2.05% and the AARD

is 0.5%. Solutions measurable at the microviscometer were also measured in the rheometer to determine the viscosity reproducibility with the two different instruments. We conducted the study primarily at 283.15 K and calculated a 2.72% MARD and 1.07% AARD.

In all our experiments, at least two measurements were taken and the average is reported as the measured property of the solution. Moreover, acid-base titration was employed to determine the samples' amine concentration also after the measurements in order to ensure no vaporization had occurred. The concentration of all samples remained unchanged even after the experiments conducted at 353.15 K.

2.3. Computational methods

Model parametrization: The parametrization procedure has been carried following the Particle Swarm Optimization (PSO) algorithm described by Ghosh et al. [41] and Poli et al.[42] and previously successfully implemented by Evjen et al. [43] and Pinto and Svendsen [43,44]. As before, the *lbest* topology was chosen with ω = 0.7298 as inertia factor and $\varphi_1 = \varphi_2$ = 1.49618 as acceleration coefficients. The objective function ϵ to be minimized is given by Eq. (1), where y is the output one is set to estimate, u is a set of input variables and θ is a set of model parameters. NP is the total number of points used for the parametrization routine.

$$\epsilon(\boldsymbol{u}, \boldsymbol{y}, \boldsymbol{\theta}) = \sum_{i=1}^{NP} \frac{(y_i - \hat{y}_i(\boldsymbol{u}, \boldsymbol{\theta}))^2}{y_i \cdot \hat{y}_i(\boldsymbol{u}, \boldsymbol{\theta})} \quad (1)$$

Furthermore, the quality of the fitting has been evaluated by two complementary criteria: the average absolute relative deviation (AARD) and the maximum absolute deviation (MAD) as defined by Eqs. (2) and (3).

$$AARD = \frac{100}{NP} \cdot \sum_{i=1}^{NP} \left| \frac{y_i - \hat{y}_i}{y_i} \right| \quad (2)$$

$$MAD = max(|\boldsymbol{y} - \hat{\boldsymbol{y}}|) \quad (3)$$

The same overall parametrization procedure has been applied both for the modeling of density and viscosity. In general lines, one initially needs to estimate the properties of single components. The properties of binaries and ternaries are then calculated by the use of a simple mixing rule plus an additional term that accounts for excess properties. In this work, the fitting is carried over the global data set, meaning that unitary, binary and ternary data sets are all coupled together in the evaluation of the objective function ϵ and accounted for in the AARD and in the MAD calculation. However, it is a good optimization practice to fit the excess property models first to each individual binary data set, thus generating a periphery of initial guesses for the fitting of the global data set. This has been the procedure carried throughout this study. A list of the symbols used in the remainder of this work is given in the nomenclature provided in the end of the manuscript.

Modeling of Density. The typical approach employed for the estimation of multicomponent system densities goes through the modeling of excess molar volumes (v^E). Once the v^E of a mixture is calculated, its density can be recovered by Eq. (4).

$$\rho = \frac{\sum_{i=1}^{NC} x_i \cdot MW_i}{v^E + \sum_{i=1}^{NC} \frac{x_i \cdot MW_i}{\rho_i}} \quad (4)$$

Following the example of Pinto et al.[45], a modified Rackett equation of the form shown in Eqs. (5) – (7) was employed for the calculation of $\hat{\rho}_i$. This calculation requires the estimation of single molar volumes in Eq. (5) by using the Rackett compressibility factor $Z_{RA,i}$ described in Eq. (6). The parameters in these equations are the critical temperature $T_{C,i}$ and critical pressure $p_{C,i}$ for each pure

146 component, plus the reduced temperature and pressure. Furthermore, three parameters ($\hat{A}_i$, $\hat{B}_i$ and $\hat{C}_i$)
147 have to be fitted for the obtention of $Z_{RA,i}$.

$$\hat{v}_i(p,T) = \frac{R \cdot T_{C,i}}{p_{C,i}} \cdot \hat{Z}_{RA,i}^{1+(1-T_{r,i})^{2/7}} \tag{5}$$

$$\hat{Z}_{RA,i}(p,T) = exp\left[\hat{A}_i + \frac{\hat{B}_i}{p_{r,i}} + \hat{C}_i \cdot ln\left(T_{r,i}\right)\right] \tag{6}$$

$$\hat{\rho}_i(p,T) = \frac{MW_i}{\hat{v}_i} \tag{7}$$

148 The estimation of the single component molar volumes $\hat{v}_i$ is followed by the estimation of the excess
149 properties $\hat{v}^E$ of binary and ternary mixtures. In the previous work carried by Evjen et al.[44], the
150 Redlich-Kister equation fulfilled this duty. However, as seen in that study, the RK equation demands
151 that at least 6 parameters are fitted for each binary mixture so that a good agreement between
152 experimental and estimated densities is obtained. These binary estimations must additionally be
153 coupled with an extra $\hat{v}^E$ model for the estimation of ternary densities[46,47]. Such correction demands
154 additional parameters and fittings in the forms proposed differently by several distinct authors, like
155 Cibulka[48], Nagata and Tamura[49], Redlich and Kister[50] and Singh et al.[51] Most of these models have at
156 least 3 extra parameters, meaning that $6 \cdot NC + 3 = 21$ empirical parameters must be found for the
157 description of the density of ternary solutions. This poses the disadvantages of having to choose one
158 among several $\hat{v}^E$ models in literature and fitting an unordinary number of coefficients. It also means
159 that the quality of the ternary data fitting is wholly dependent on the quality of the binary data fitting.

160 An alternative to this has been suggested by Pinto and Knuutila[52] for the direct fitting of ternary
161 density data. This model, henceforth called the NRTL-DVOL, is explicitly based on the non-random
162 two liquid (NRTL) model and has the form outlined in Eqs. (8) – (11).

$$\hat{v}^E(\boldsymbol{x},T) = R \cdot T \cdot \sum_{i=1}^{NC} x_i \cdot \frac{\sum_{j=1}^{NC} \hat{\tau}_{ji} \cdot \hat{G}_{ji} \cdot x_j}{\sum_{k=1}^{NC} \hat{G}_{ki} \cdot x_k} \quad (8)$$

$$\hat{G}_{ij}(T) = exp\left(-\alpha_{ij} \cdot \hat{\tau}_{ij}\right) \quad (9)$$

$$\hat{\tau}_{ij}(T) = \hat{a}_{ij} + \frac{\hat{b}_{ij}}{T} \quad (10)$$

$$\hat{a}_{ii} = 0\,;\ \hat{b}_{ii} = 0\,;\ \hat{\alpha}_{ij} = \hat{\alpha}_{ji} \quad (11)$$

The expressions shown in Eqs. (8) – (11) demand the fitting of $\hat{a}_{ij}$ and $\hat{b}_{ij}$. Meanwhile, R is a fixed parameter of the model and its value is R = 6.48803. The non-randomness parameter α_{ij} is set alternatively at α_{ij} = 0.1, 0.2 or 0.3, and the optimization routines are performed once for each of these values. In the present work, a global $\alpha_{ij} = \alpha$ was implemented for each study, meaning that a single $\hat{\alpha}$ was chosen for the binary-ternary systems instead of one for each binary.

Modeling of Viscosity.

Similar to density, the modelling of the viscosity requires the "excess viscosity" of the mixture, or more correctly the viscosity deviations from ideality upon mixture. In this work, viscosity deviations $\Delta\eta$ were calculated from the experimental measurements using Eqs. (12)-(13)[53,54]:

$$ln\left(\eta^{id}\right) = \sum_{i=1}^{NC} x_i \cdot ln(\eta_i) \quad (12)$$

$$\Delta\eta = \eta - \eta^{id} \quad (13)$$

where η^{id} is the viscosity of the ideal mixture, x_i and η_i are the molar fraction and viscosity of the pure component i respectively, η is the measured viscosity of the mixture and $\Delta\eta$ is the viscosity deviation upon mixing.

There are several approaches for modeling the viscosity of binary liquid mixtures. However, only the models of Song et al.[55] and Pinto and Svendsen[43] offer an easy extension towards the calculation of ternary mixtures. The former is usually called the Aspen liquid mixture viscosity model, whereas the latter was baptized the NRTL-DVIS model. Both of them are reliant on good estimatives of pure component viscosities. Therefore, the viscosities of pure MDEA and MEG were fitted to the Vogel equation, which has a generic form shown in Eq. (14).

$$ln(\hat{\eta}_i(T)) = \hat{A}_i + \frac{\hat{B}_i}{T - \hat{C}_i} \tag{14}$$

Meanwhile, the viscosity of pure water can be estimated by the correlation of Bingham and Jackson[56] given in Eqs. (15) – (16).

$$\varphi_{H2O}(T) = 2.1482 \cdot \left[(T - 281.585) + \sqrt{8078.4 + (T - 281.585)^2}\right] - 120 \tag{15}$$

$$\hat{\eta}_{H2O}(T) = \frac{100}{\varphi_{H2O}} \tag{16}$$

The viscosity of mixtures is estimated by the addition of an excess viscosity term, different from the one displayed in Eqs. (12) – (13), as shown in Eq. (17). Following the initial suggestion of Song et al.[55], the mass fractions w_i are better weights for the mixture calculations than the molar fractions x_i.

$$ln(\hat{\eta}(\boldsymbol{w}, T)) = \sum_{i=1}^{NC} w_i \cdot ln(\hat{\eta}_i(T)) + ln(\hat{\eta}^E(\boldsymbol{w}, T)) \tag{17}$$

Moreover, the form that this excess term $\hat{\eta}^E$ can take is what differs the Aspen liquid mixture viscosity model from the NRTL-DVIS model. Following the Aspen liquid mixture viscosity model, this term is calculated by the Eqs. (18) – (21). These equations require that four different set of parameters, $\hat{a}_{ij}$, $\hat{b}_{ij}$, $\hat{c}_{ij}$ and $\hat{d}_{ij}$, are estimated for each binary pair.

$$ln(\hat{\eta}^E(\boldsymbol{w},T)) = \sum_{i=1}^{NC}\sum_{j>i}^{NC} \hat{k}_{ij} \cdot w_i \cdot w_j \cdot ln(\hat{\eta}_{ij}) + \sum_{i=1}^{NC} w_i \left[\cdot \sum_{j\neq i}^{NC} w_j \cdot \left(\hat{l}_{ij} \cdot ln(\hat{\eta}_{ij})\right)^{1/3} \right]^3 \quad (18)$$

$$ln(\hat{\eta}_{ij}) = \frac{\left|ln(\hat{\eta}_i) - ln(\hat{\eta}_j)\right|}{2} \quad (19)$$

$$\hat{k}_{ij}(T) = \hat{a}_{ij} + \frac{\hat{b}_{ij}}{T} \quad (20)$$

$$\hat{l}_{ij}(T) = \hat{c}_{ij} + \frac{\hat{d}_{ij}}{T} \quad (21)$$

Similarly, the NRTL-DVIS model also requires that 12 parameters be estimated. Its form is very similar to that of the NRTL-DVOL, since both come from the same approach of modeling excess properties with the general shape of the NRTL excess Gibbs energy equation. The model is described by the Eqs. (22) – (25).

$$ln(\hat{\eta}^E(\boldsymbol{w},T)) = R \cdot \sum_{i=1}^{NC} w_i \cdot \frac{\sum_{j=1}^{NC} \hat{\tau}_{ji} \cdot \hat{G}_{ji} \cdot w_j}{\sum_{k=1}^{NC} \hat{G}_{ki} \cdot w_k} \quad (22)$$

$$\hat{G}_{ij}(T) = exp\left(-\alpha_{ij} \cdot \hat{\tau}_{ij}\right) \quad (23)$$

$$\hat{\tau}_{ij}(T) = \hat{a}_{ij} + \frac{\hat{b}_{ij}}{T} \quad (24)$$

$$\hat{a}_{ii} = 0\ ;\ \hat{b}_{ii} = 0\ ;\ \hat{\alpha}_{ij} = \hat{\alpha}_{ji} \quad (25)$$

All of the remarks made regarding the NRTL-DVOL apply to the NRTL-DVIS model. Once again a value of R = 6.48803 was set as a fixed parameter of the equations, whereas $\alpha_{ij} = \alpha$ was set alternatively to α = 0.1, 0.2 and 0.3 for each optimization routine.

3. RESULTS AND DISCUSSION

The results of density ρ and viscosity η measurements and modeling for the binary mixtures of MDEA-MEG and the ternary mixtures of MDEA-MEG-H_2O are presented below.

3.1. Density

The density of pure water, monoethylene glycol and methyldiethanolamine was measured and compared to values from the literature for validation purposes. Our measured densities were compared against the literature sources presented in **Table 1** and, to be more specific, against data reported by Bernal-Garcia et al.[10], Hayduk and Malik[21], Yang et al.[24], Tsierkezos and Molinou[25] and Spieweck and Bettin[57] for water, data reported by Hayduk and Malik[21], Bohne et al.[22], Afzal et al.[26], Yang et al.[24] and Tsierkezos and Molinou[25] for MEG and data reported by Bernal-Garcia et al.[10], Al-Ghawas et al.[11], Alvarez et al.[32], Paul and Mandal[13] and Yin et al.[14] for MDEA. The average absolute relative deviation (AARD) is 0.01% for water, 0.30% for MEG and 0.10% for MDEA, demonstrating that our measurements are in good agreement with the data already reported in the literature. Indicative literature data sets are given in **Table 3**, selected because they cover as many temperatures studied in this work as possible. The AARD using those two sources for each component was found to be 0.03%, 0.33% and 0.12% for water, MEG and MDEA respectively.

215 **Table 3:** Experimental and Indicative Literature Values of Density ρ/kg·m^{-3} for Pure Water, MEG and MDEA at Temperatures T =
216 (283.15 – 353.15) K and Pressure near p = 0.1 MPa

	ρ / kg·m^{-3}								
	Water			MEG			MDEA		
T / K	Spieweck & Bettin[57]	Yang et al.[24]	This work	Afzal et al.[26]	Yang et al.[24]	This work	Bernal-Garcia et al.[10]	Al-Ghawas et al.[11]	This work
283.15	999.699	-	999.9	1120.23	-	1120.0	1047.53	-	1048.0
298.15	997.043	-	997.2	1109.77	-	1109.9	1037.86	1037.4	1036.8
313.15	992.212	992.2	992.3	1099.17	1093.6	1098.8	1026.52	1026.7	1025.4
323.15	988.030	988.1	988.3	1092.02	1084.7	1091.6	1018.88	1019.4	1017.7
333.15	983.191	983.2	983.5	1084.78	1076.4	1085.0	1011.43	1012.3	1010.0
343.15	977.759	977.8	978.1	1077.42	1067.5	1077.6	1003.32	-	1002.2
353.15	971.785	971.8	972.3	1069.95	1060.0	1070.1	995.41	-	994.6
AARD[a]			**0.03%**			**0.33%**			**0.12%**

217 [a] $AARD\ [\%] = \frac{100}{NP}\sum_{i=1}^{NP}\left|\frac{\rho_i^{exp} - \rho_i^{lit}}{\rho_i^{lit}}\right|$

Table 4 and **Table 5** show the measured densities in this work for the non-aqueous and aqueous MEG-MDEA mixtures respectively as a function of weight fraction w and temperature T at ambient pressure. The expanded uncertainties with a 0.95 level of confidence of composition and density are provided for each system and temperature. In addition to the weight fractions, molar fractions x_i and the corresponding uncertainties can be found in Supporting Information. As mentioned earlier, the repeatability of the density measurements is excellent, as one can see in the results. It is observed that the density of the binary mixtures of MDEA-MEG decreases with temperature and with MDEA concentration. These trends are better illustrated in **Figure 1**, presenting the experimental densities for the binary system MDEA-MEG and the estimates generated by the NRTL-DVOL model. Similar figures for MDEA-H_2O and MEG-H_2O are provided in Supporting Information. The density of MEG-H_2O is similar to the one for MDEA-MEG while the one for the binary MDEA-H_2O varies in the way that it increases with MDEA concentration, but only up to approximately $w_1 = 0.7$ after which it starts decreasing. This behavior is due to the excess molar volumes upon mixture of MDEA and H_2O and is discussed in detail under subsection *3.3 Excess Properties*. The trend of decreasing density with temperature and amine content apply for the ternary systems as well, given that the amount of water in the solution is constant. The generated density contour plots for the ternary system can be found in Supporting Information.

Table 4: Experimental Values of Density ρ/kg·m^{-3} for {MDEA (1) + MEG (2)} as a Function of Weight Fraction w and Temperature T at Pressure p = 0.1020 MPa[a]

w_1	ρ / kg·m^{-3}					
	283.15 K	298.15 K	313.15 K			
	Set A	Set A	Set A (1)	Set A (2)	Set A (3)	Set C
0.000	1120.0 ± 0.2	1109.9 ± 0.3	1098.8 ± 0.3	1099.3 ± 0.3	-	1099.3 ± 0.3
0.300 ± 0.003	1101.8 ± 0.2	1090.9 ± 0.2	1079.9 ± 0.1	1079.9 ± 0.1	1079.9 ± 0.1	1080.0 ± 0.1
0.400 ± 0.003	1095.1 ± 0.2	1084.3 ± 0.2	1073.2 ± 0.1	1073.2 ± 0.1	-	-
0.500 ± 0.004	1088.1 ± 0.2	1077.2 ± 0.2	1066.0 ± 0.1	1066.0 ± 0.1	-	-
0.700 ± 0.006	1073.3 ± 0.2	1062.1 ± 0.2	1050.7 ± 0.1	1050.8 ± 0.1	-	-
0.800 ± 0.008	1065.4 ± 0.2	1054.0 ± 0.2	1042.5 ± 0.1	1042.6 ± 0.1	-	-
0.900 ± 0.009	1057.2 ± 0.2	1045.6 ± 0.2	1034.1 ± 0.1	1034.1 ± 0.1	1034.1 ± 0.1	1034.0 ± 0.1
1.000 ± 0.011	1048.0 ± 0.2	1036.8 ± 0.2	1025.4 ± 0.1	1025.4 ± 0.1	-	1025.1 ± 0.1

w_1	323.15 K	333.15 K		
	Set A	Set A (1)	Set A (2)	Set C
0.000	1091.6 ± 0.1	1085.0 ± 0.1	-	1084.9 ± 0.1
0.300 ± 0.003	1072.5 ± 0.1	1065.1 ± 0.1	1065.0 ± 0.1	1065.2 ± 0.1
0.400 ± 0.003	1065.7 ± 0.1	1058.1 ± 0.1	-	-
0.500 ± 0.004	1058.5 ± 0.1	1050.9 ± 0.1	-	-
0.700 ± 0.006	1043.1 ± 0.1	1035.4 ± 0.1	-	-
0.800 ± 0.008	1034.9 ± 0.1	1027.2 ± 0.1	-	-
0.900 ± 0.009	1026.4 ± 0.1	1018.7 ± 0.1	1018.7 ± 0.1	1018.6 ± 0.1
1.000 ± 0.011	1017.7 ± 0.1	1010.0 ± 0.1	-	1010.0 ± 0.1

w_1	343.15 K	353.15 K		
	Set A	Set A (1)	Set A (2)	Set C
0.000	1077.6 ± 0.1	1070.1 ± 0.1		1070.1 ± 0.1
0.300 ± 0.003	1057.4 ± 0.1	1049.7 ± 0.1		1049.7 ± 0.1
0.400 ± 0.003	1050.5 ± 0.1	1042.7 ± 0.1		1042.7 ± 0.1
0.500 ± 0.004	1043.1 ± 0.1	1035.3 ± 0.1		1035.3 ± 0.1
0.700 ± 0.006	1027.5 ± 0.1	1019.7 ± 0.1		1019.7 ± 0.1
0.800 ± 0.008	1019.3 ± 0.1	1011.5 ± 0.1		1011.5 ± 0.1
0.900 ± 0.009	1010.9 ± 0.1	1003.1 ± 0.1		1003.1 ± 0.1
1.000 ± 0.011	1002.2 ± 0.1	994.6 ± 0.1		994.6 ± 0.1

[a]Weight fractions and densities are reported with their expanded uncertainties (0.95 level of confidence). Expanded uncertainties not included above are $U(T) = 0.02$ K and $U(p) = 0.0030$ MPa.

Table 5: Experimental Values of Density ρ/kg·m^{-3} for {MDEA (1) + MEG (2) + Water (3)} as a Function of Weight Fraction w and Temperature T at Pressure p = 0.1020 MPa[a]

w_1	w_2	ρ / kg·m^{-3}				
		283.15 K	298.15 K	313.15 K	323.15 K	333.15 K
		Set A	Set A	Set A	Set A	Set A
0.050 ± 0.002	0.900 ± 0.003	1114.1 ± 0.2	1103.7 ± 0.3	1093.1 ± 0.1	1086.4 ± 0.6	1079.1 ± 0.7
0.900 ± 0.013	0.050 ± 0.010	1057.6 ± 0.2	1046.3 ± 0.3	1034.8 ± 0.1	1027.5 ± 0.6	1019.8 ± 0.7
0.300 ± 0.003	0.600 ± 0.003	1196.6 ± 0.2	1086.1 ± 0.3	1075.1 ± 0.1	1068.2 ± 0.6	1060.7 ± 0.7
0.600 ± 0.006	0.300 ± 0.006	1078.5 ± 0.2	1067.6 ± 0.3	1056.3 ± 0.1	1049.1 ± 0.6	1041.5 ± 0.7
0.100 ± 0.002	0.600 ± 0.002	1090.1 ± 0.2	1080.5 ± 0.3	1070.3 ± 0.1	1063.4 ± 0.6	1056.8 ± 0.7
0.300 ± 0.003	0.400 ± 0.003	1081.2 ± 0.2	1071.2 ± 0.3	1060.9 ± 0.1	1053.8 ± 0.6	1047.1 ± 0.7
0.600 ± 0.006	0.100 ± 0.006	1067.8 ± 0.2	1057.4 ± 0.3	1046.5 ± 0.1	1039.4 ± 0.6	1031.7 ± 0.7
0.250 ± 0.002	0.250 ± 0.002	1061.0 ± 0.2	1052.2 ± 0.3	1043.2 ± 0.1	1036.6 ± 0.6	1030.5 ± 0.7

w_1	w_2	343.15 K	353.15 K		
		Set A	Set A (1)	Set A (2)	Set C
0.050 ± 0.002	0.900 ± 0.003	1071.8 ± 0.7	1064.5 ±0.9	1064.6 ±0.9	-
0.900 ± 0.013	0.050 ± 0.010	1012.0 ± 0.7	1004.2 ±0.9	1004.2 ±0.9	-
0.300 ± 0.003	0.600 ± 0.003	1053.2 ± 0.7	1045.6 ±0.9	1045.7 ±0.9	1045.7 ±0.9
0.600 ± 0.006	0.300 ± 0.006	1033.6 ± 0.7	1025.8 ±0.9	1025.8 ±0.9	-
0.100 ± 0.002	0.600 ± 0.002	1049.4 ± 0.7	1042.0 ±0.9	1042.2 ±0.9	-
0.300 ± 0.003	0.400 ± 0.003	1039.5 ± 0.7	1031.8 ±0.9	1031.9 ±0.9	-
0.600 ± 0.006	0.100 ± 0.006	1023.7 ± 0.7	1015.7 ±0.9	1015.8 ±0.9	-
0.250 ± 0.002	0.250 ± 0.002	1023.5 ± 0.7	1016.1 ±0.9	1016.1 ±0.9	1016.2 ±0.9

[a]Weight fractions and densities are reported with their expanded uncertainties (0.95 level of confidence). Expanded uncertainties not included above are $U(T)$ = 0.02 K and $U(p)$ = 0.0030 MPa.

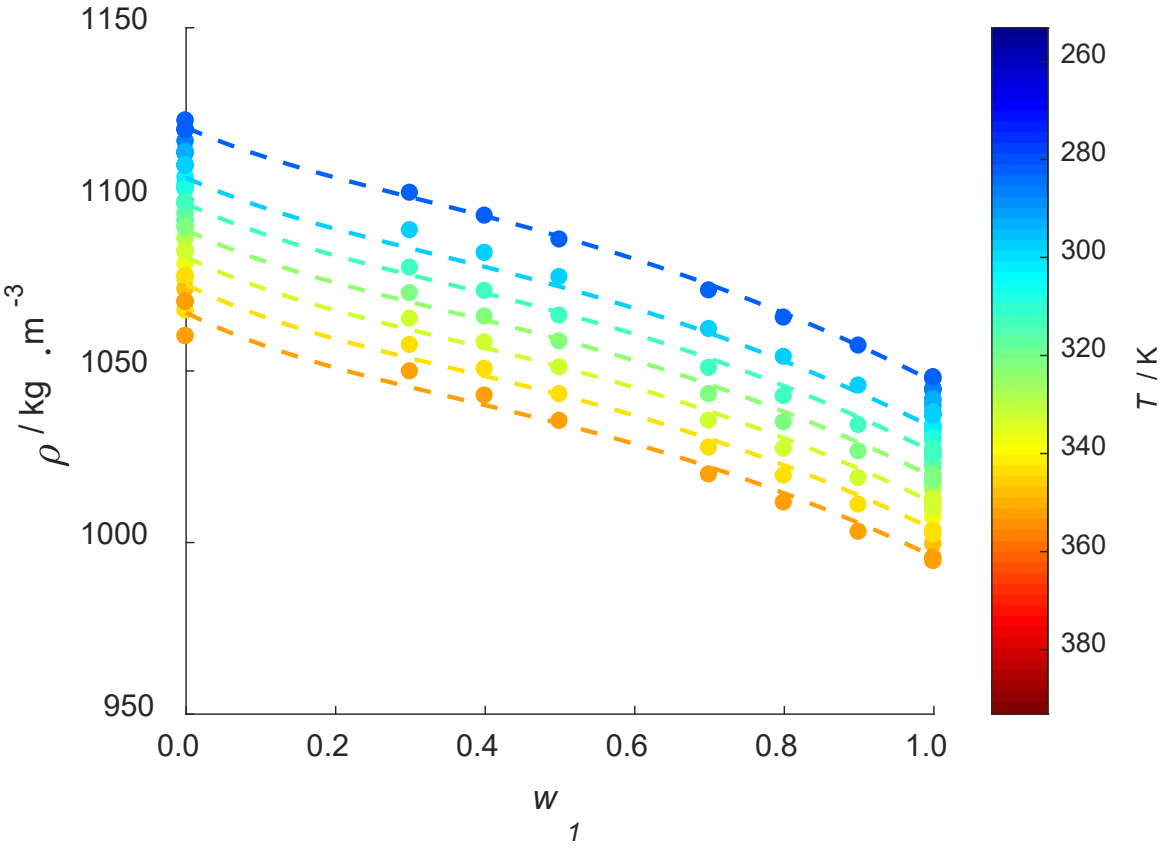

Figure 1. Binary data set of densities for {MDEA (1) + MEG (2)} and estimations generated by the NRTL-DVOL model. The temperature in which each experimental point (●) was measured is color-coded by the bar on the right side. The temperatures in which the estimates were made were 283.15 K (dark blue dashed line), 298.15 K (capri blue dashed line), 313.15 K (aqua dashed line), 323.15 K (green dashed line), 333.15 K (lime green dashed line), 343.15 K (yellow dashed line) and 353.15 K (orange dashed line).

As explained in the Experimental and Computational Methods, a modified Rackett equation was employed for the fitting of the single component data sets shown in **Table 1**. The results of the fitting are presented in **Table 6** and **Figure 2.** The values of MW, T_C and p_C were obtained from Yaws[58].

The fitting for water was not performed in this study, but the parameters for its modified Rackett equation were obtained from Pinto and Knuutila[52]. As such, we merely report the parameters obtained by these authors without checking their significance – though it should be pointed out that the parameter $\hat{B}$ obtained by Pinto and Knuutila[52] of $6.6495 \cdot 10^{-6}$ could be set to zero with no noticeable effects to the performance of the model. Though the results for the fitting of MEG are worse than those of MDEA, this is arguably due to the scatter in experimental data found for MEG in the literature, as evidenced by **Figure 2**. The density data of pure MEG reported by Yang et al.[24] is partially responsible for this scatter, as their values are consistently lower than those obtained by other researchers (see bifurcation in the blue data points in **Figure 2**), particularly at higher temperatures. However, the data set from Yang et al.[24] contains pure water density measurements in excellent agreement with literature, and their collection of pure MEG density measurements are off by only 1% when compared to other published data. Therefore, we have decided to keep their data set in our parametrization procedure.

Table 6. Parameters and results for the fittings of the modified Rackett equation

Parameter	MDEA	MEG	Water[52]
MW (kg·kmol^{-1})	119.16	62.07	18.02
T_C (K)	675	720	647.1
p_C (MPa)	3.88	8.20	22.064
$\hat{A}$	-1.4003	-1.4021	-1.4937
$\hat{B}$	$-3.0132 \cdot 10^{-6}$	$-0.7670 \cdot 10^{-6}$	$6.6495 \cdot 10^{-6}$
$\hat{C}$	-0.03542	-0.02230	-9.868
$AARD$ (%)	0.07	0.19	0.35
MAD (kg·m^{-3})	2.36	7.68	15.82

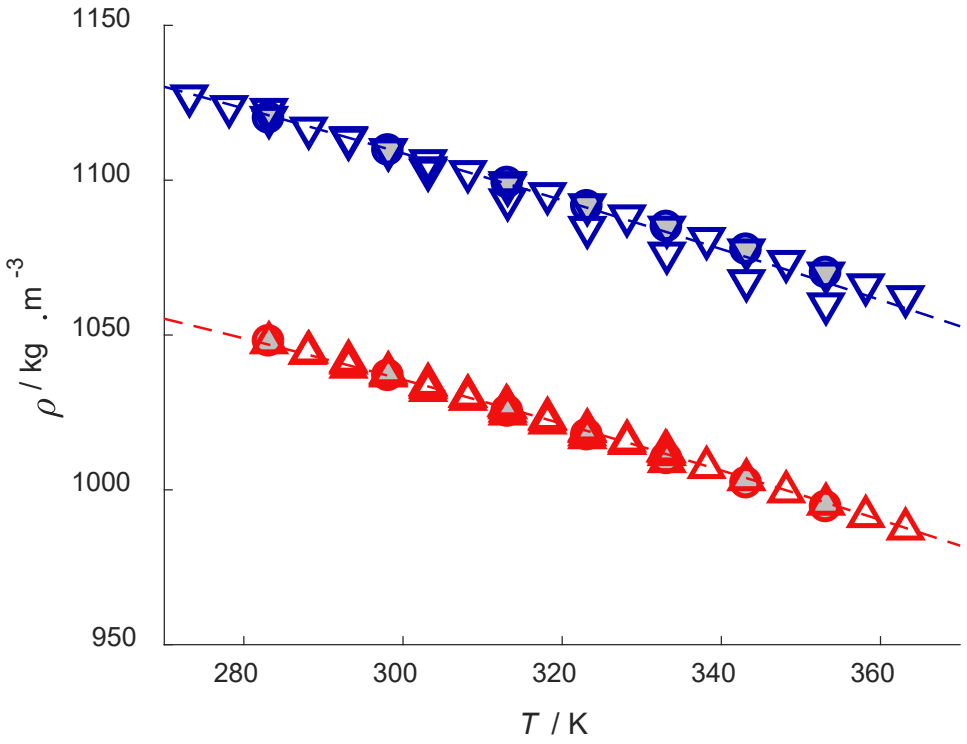

Figure 2. Experimental single component density of MDEA both obtained in literature (red Δ) as produced in this work (red ○ filled in grey) and of MEG both obtained in literature (blue ∇) as produced in this work (blue ○ filled in grey), plus corresponding estimations with the modified Rackett equation for MDEA (red dashed line) and MEG (blue dashed line).

Table 7 shows the results for the fitting with the NRTL-DVOL model. The fitting was done by minimizing the objective function Eq. (1) with the entire data set of unitary, binary and ternary solutions. Moreover, since the parameters found for the NRTL-DVOL fitting are valid for estimating binary as well as ternary data, **Table 7** shows first the AARD and MAD obtained for the binaries and then that obtained for the global data set. It can be seen that the AARDs are very small for the three binaries and that the deviations for the MEG-water binary case are the worst. This will be discussed

278 further with **Figure 3**. Overall, the fitting results are quite good and show that the densities of both
279 binary and ternary mixtures can be estimated with a high degree of confidence.

280 **Table 7.** Parameters and results for the NRTL-DVOL equation fitted for the global data set

Parameters of the NRTL-DVOL model (1 = MDEA, 2 = MEG, 3 = water)					
$\hat{a}_{12}$	-0.59445	$\hat{a}_{13}$	-0.77567	$\hat{a}_{23}$	0.44978
$\hat{a}_{21}$	0.63227	$\hat{a}_{31}$	0.83786	$\hat{a}_{32}$	-0.44286
$\hat{b}_{12}$	-20.026	$\hat{b}_{13}$	-24.830	$\hat{b}_{23}$	-118.93
$\hat{b}_{21}$	21.832	$\hat{b}_{31}$	29.961	$\hat{b}_{32}$	117.49
$\alpha_{ij} = \alpha = 0.1$; $R = 6.48803$					
Fitting results in terms of binary data sets					
MDEA-MEG		MDEA-water		MEG-water	
$AARD$ (%)	0.14	$AARD$ (%)	0.16	$AARD$ (%)	0.38
MAD (kg·m^{-3})	7.68	MAD (kg·m^{-3})	5.63	MAD (kg·m^{-3})	28.75
Fitting results in terms of the global data set					
$AARD$ (%)	0.26				
MAD (kg·m^{-3})	28.75				

281

The parity plots exhibited in **Figure 3 (a) and (b)** reinforce that the fitting of the NRTL-DVOL model for the global data set is good, with only a few remarkable features. One of them is the higher deviations observed for binary data regarding MEG-water mixtures (cyan ×), which account for the largest share in the decoupling between model and experimental data. **Figure 3 (a)** evidences that this decoupling is the strongest at lower densities or, conversely, higher temperatures (**Figure 3 (b)**). This can be explained by the scatter of data points at these specific conditions and by the original scatter of pure MEG data observed already in **Figure 2**. Other decoupling trends, such as that for MDEA-water binary mixtures at higher temperatures (green *), are an unfortunate consequence of fitting parameters for such a wide range of temperatures and compositions. Nevertheless, for all systems, besides one MEG-water data point, the deviations are not higher than 1%. One can also observe the absolute relative deviations (ARDs) between measured and estimated values for ternary systems in Table S1 in the Supporting Information.

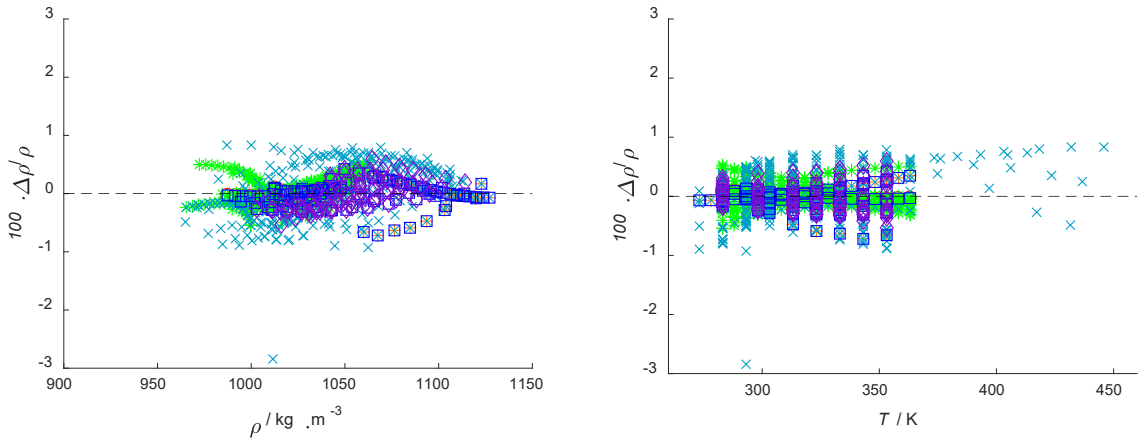

(a) (b)

Figure 3. Deviations in terms of differences between experimental and estimated densities divided by experimental densities regarding estimations made with the NRTL-DVOL model, and how they vary the experimental densities themselves (a) and with temperature (b). The data sets are distributed in

299 terms of pure MDEA data (red ○), pure MEG data (orange +), binary MDEA-water data (green *),

300 binary MEG-water data (cyan ×), binary MDEA-MEG data (blue □) and ternary data (purple ◊).

3.2. Viscosity

The viscosity of pure water, monoethylene glycol and methyldiethanolamine was measured and compared to values from the literature for validation purposes. At temperatures higher than 323.15 K it was not possible to measure the viscosity of pure water. Similar to the density study, our measured viscosities were compared against all the literature sources presented in **Table 1**. The data used for the validation are from Teng et al.[15], Bernal-Garcia et al.[16], Chowdhury et al.[18], Pinto et al.[17], Li and Lie[12] and Yin et al.[14] for MDEA, and from Hayduk and Malik[21], Bohne et al.[22], Tsierkezos and Molinou[25], Yang et al.[24], Jerome et al.[37] and Dunstan[38] for MEG. For water, the same references as previously mentioned for MEG validation were used, in addition to Teng et al.[15], Bernal-Garcia et al.[16] and Chowdhury et al.[18]. The AARDs are 2.40%, 3.78% and 2.71% for water, MEG and MDEA respectively. The AARDs for viscosity are higher than for density, indicating the more challenging nature of viscosity measurements compared to the density ones. The data obtained agree satisfactorily with the data already reported in the literature, with the exception of pure MEG at 283.15 K. Indicative reference sources and their corresponding AARDs are given in **Table 8**.

315 **Table 8:** Experimental and Indicative Literature Values of Viscosity η/mPa·s for pure water, MEG and MDEA at Temperatures T =
316 (283.15 – 353.15) K and Pressure near p = 0.1 MPa

	η / mPa·s									
	water			MEG				MDEA		
T / K	IAPWS 2008[59]	Yang et al.[24]	This work	Tsierkezos & Molinou[25]	Bohne et al.[22]	Yang et al.[24]	This work	Teng et al.[15]	Li & Lie[12]	This work
283.15	1.3059	-	1.32	30.5126	-	-	34.07	-	-	198.15
298.15	0.8900	-	0.91	-	16.630	-	17.27	77.190	-	75.37
313.15	0.6527	0.653	0.67	9.5348	9.407	9.443	9.69	34.110	34.3085	35.05
323.15	0.5465	0.547	0.57	-	-	6.992	6.81	-	21.6716	21.96
333.15	-	-	-	-	5.030	5.06	5.28	14.300	14.3856	14.83
343.15	-	-	-	-	-	3.987	4.06	9.849	9.9789	10.29
353.15	-	-	-	-	3.068	3.021	3.21	7.115	7.0875	7.40
AARD[a]			**2.79%**				**4.30%**			**3.15%**

317 [a] $AARD\ [\%] = \frac{100}{NP}\sum_{i=1}^{NP}\left|\frac{\eta_i^{exp} - \eta_i^{lit}}{\eta_i^{lit}}\right|$

318 The measured viscosities for the non-aqueous and aqueous MDEA-MEG and corresponding
319 expanded uncertainties with a 0.95 level of confidence are shown in **Table 9** and **Table 10**
320 respectively. The repeatability of density measurements was excellent, while the one for viscosity is
321 lower, though still satisfactory. As presented earlier in *2. Experimental and Computational Methods*
322 section, Set A consists of the measurements conducted in the microviscometer, Set B consists of the
323 ones conducted in the rheometer and Set C includes all the measurements performed to study the
324 reproducibility of the obtained data.

325 **Table 9:** Experimental Values of Viscosity η/mPa·s for {MDEA (1) + MEG (2)} as a Function of Weight Fraction w and Temperature
326 T at Pressure p = 0.1020 MPa[a]

		η / mPa·s		
T /K	w_1	Set A	Set B (1)	Set B (2)
283.15	0.000	34.40 ± 4.52	33.92 ± 4.06	33.88 ± 4.06
	0.300 ± 0.003	-	64.34 ± 4.10	64.37 ± 4.10
	0.400 ± 0.003	-	80.69 ± 4.06	80.69 ± 4.06
	0.500 ± 0.004	-	99.66 ± 4.08	-
	0.700 ± 0.006	-	-	-
	0.800 ± 0.008	-	164.27 ± 4.27	-
	0.900 ± 0.009	-	181.33 ± 4.42	-
	1.000 ± 0.011	-	197.93 ± 4.20	198.37 ± 4.20

T /K	w_1	Set A	Set B (1)	Set B (2)
298.15	0.000	17.28 ± 1.08	-	17.25 ± 1.08
	0.300 ± 0.003	30.43 ± 1.08	-	-
	0.400 ± 0.003	36.57 ± 1.08	-	-
	0.500 ± 0.004	43.44 ± 1.09	43.65 ± 2.61	-
	0.700 ± 0.006	-	58.07 ± 2.61	-
	0.800 ± 0.008	-	66.59 ± 2.62	-
	0.900 ± 0.009	-	69.21 ± 2.61	-
	1.000 ± 0.011	-	75.87 ± 2.62	74.87 ± 1.08

T /K	w_1	Set A (1)	Set A (2)	Set A (3)	Set B	Set C
313.15	0.000	9.42 ± 1.06	9.82 ± 1.06	-	-	9.83 ± 1.06

	0.300 ± 0.003	15.74 ± 1.04	15.87 ± 1.04	15.87 ± 1.04	-	16.07 ± 1.04
	0.400 ± 0.003	18.43 ± 1.04	18.61 ± 1.04	-	-	-
	0.500 ± 0.004	21.20 ± 1.06	21.58 ± 1.06	-	21.97 ± 0.49	-
	0.700 ± 0.006	27.33 ± 1.07	27.96 ± 1.07	27.88 ± 1.07	-	-
	0.800 ± 0.008	30.30 ± 1.06	30.68 ± 1.06	-	-	-
	0.900 ± 0.009	32.80 ± 1.06	33.38 ± 1.06	33.23 ± 1.06	32.39 ± 0.48	33.46 ± 1.06
	1.000 ± 0.011	34.82 ± 1.07	35.30 ± 1.07	-	34.99 ± 0.48	35.07 ± 1.07

T /K	w_1	Set A
323.15	0.000	6.81 ± 0.36
	0.300 ± 0.003	10.80 ± 0.34
	0.400 ± 0.003	12.43 ± 0.34
	0.500 ± 0.004	14.20 ± 0.34
	0.700 ± 0.006	17.75 ± 0.34
	0.800 ± 0.008	19.48 ± 0.34
	0.900 ± 0.009	20.91 ± 0.34
	1.000 ± 0.011	21.96 ± 0.38

T /K	w_1	Set A (1)	Set A (2)	Set C
333.15	0.000	5.26 ± 0.47	-	5.30 ± 0.47
	0.300 ± 0.003	7.76 ± 0.47	7.82 ± 0.47	7.88 ± 0.47
	0.400 ± 0.003	8.82 ± 0.47	-	-
	0.500 ± 0.004	9.94 ± 0.47	-	-
	0.700 ± 0.006	12.17 ± 0.47	-	-
	0.800 ± 0.008	13.26 ± 0.47	-	-

	0.900 ± 0.009	14.08 ± 0.47	14.16 ± 0.47	14.13 ± 0.47
	1.000 ± 0.011	14.76 ± 0.47	-	14.90 ± 0.47

T /K	w_1	Set A
343.15	0.000	4.06 ± 0.46
	0.300 ± 0.003	5.75 ± 0.46
	0.400 ± 0.003	6.45 ± 0.46
	0.500 ± 0.004	7.17 ± 0.46
	0.700 ± 0.006	8.61 ± 0.46
	0.800 ± 0.008	9.26 ± 0.46
	0.900 ± 0.009	9.81 ± 0.46
	1.000 ± 0.011	10.29 ± 0.53

T /K	w_1	Set A (1)	Set A (2)	Set C
353.15	0.000	3.20 ± 0.31	-	3.22 ± 0.31
	0.300 ± 0.003	4.44 ± 0.31	4.43 ± 0.31	4.46 ± 0.31
	0.400 ± 0.003	4.89 ± 0.31	-	-
	0.500 ± 0.004	5.36 ± 0.31	-	-
	0.700 ± 0.006	6.32 ± 0.31	-	-
	0.800 ± 0.008	6.76 ± 0.31	-	-
	0.900 ± 0.009	7.12 ± 0.31	7.13 ± 0.31	7.13 ± 0.31
	1.000 ± 0.011	7.42 ± 0.31	7.37 ± 0.31	7.42 ± 0.31

[a]Weight fractions and viscosities are reported with their expanded uncertainties (0.95 level of confidence). Expanded uncertainties not included above are $U(T)$ = 0.02 K and $U(p)$ = 0.0030 MPa.

329 **Table 10:** Experimental Values of Viscosity η/mPa·s for {MDEA (1) + MEG (2) + Water (3)} as a Function of Weight Fraction w and
330 Temperature T at Pressure p = 0.1020 MPa[a]

			η / mPa·s		
T /K	w_1	w_2	Set A	Set B (1)	Set B (2)
283.15	0.050 ± 0.002	0.900 ± 0.003	30.86 ± 4.52	30.06 ± 4.08	30.67 ± 4.08
	0.900 ± 0.013	0.050 ± 0.010	-	201.93 ± 5.06	206.07 ± 5.06
	0.300 ± 0.003	0.600 ± 0.003	47.03 ± 4.53	47.20 ± 4.07	-
	0.600 ± 0.006	0.300 ± 0.006	-	103.16 ± 4.60	-
	0.100 ± 0.002	0.600 ± 0.002	13.13 ± 4.52	12.93 ± 4.06	12.95 ± 4.06
	0.300 ± 0.003	0.400 ± 0.003	22.48 ± 4.52	22.26 ± 4.06	22.37 ± 4.06
	0.600 ± 0.006	0.100 ± 0.006	58.83 ± 4.53	58.74 ± 4.07	58.74 ± 4.07
	0.250 ± 0.002	0.250 ± 0.002	9.61 ± 4.52	9.91 ± 4.06	9.73 ± 4.06
T /K	w_1	w_2	Set A (1)	Set A (2)	Set B
298.15	0.050 ± 0.002	0.900 ± 0.003	15.80 ± 1.08	-	-
	0.900 ± 0.013	0.050 ± 0.010	-	-	79.59 ± 2.61
	0.300 ± 0.003	0.600 ± 0.003	22.51 ± 1.08	22.43 ± 1.08	-
	0.600 ± 0.006	0.300 ± 0.006	43.92 ± 1.08	-	-
	0.100 ± 0.002	0.600 ± 0.002	7.27 ± 1.08	-	-
	0.300 ± 0.003	0.400 ± 0.003	11.52 ± 1.08	-	-
	0.600 ± 0.006	0.100 ± 0.006	25.09 ± 1.08	-	-
	0.250 ± 0.002	0.250 ± 0.002	5.35 ± 1.08	5.30 ± 1.08	-
T /K	w_1	w_2	Set A		

313.15	0.050 ± 0.002	0.900 ± 0.003	9.02 ± 1.04
	0.900 ± 0.013	0.050 ± 0.010	34.90 ± 1.04
	0.300 ± 0.003	0.600 ± 0.003	12.01 ± 1.04
	0.600 ± 0.006	0.300 ± 0.006	20.96 ± 1.04
	0.100 ± 0.002	0.600 ± 0.002	4.40 ± 1.04
	0.300 ± 0.003	0.400 ± 0.003	6.44 ± 1.04
	0.600 ± 0.006	0.100 ± 0.006	12.15 ± 1.04
	0.250 ± 0.002	0.250 ± 0.002	3.25 ± 1.04

T /K	w_1	w_2	Set A
323.15	0.050 ± 0.002	0.900 ± 0.003	6.49 ± 0.34
	0.900 ± 0.013	0.050 ± 0.010	21.70 ± 0.34
	0.300 ± 0.003	0.600 ± 0.003	8.32 ± 0.34
	0.600 ± 0.006	0.300 ± 0.006	13.60 ± 0.34
	0.100 ± 0.002	0.600 ± 0.002	3.36 ± 0.34
	0.300 ± 0.003	0.400 ± 0.003	4.73 ± 0.34
	0.600 ± 0.006	0.100 ± 0.006	8.18 ± 0.34
	0.250 ± 0.002	0.250 ± 0.002	2.46 ± 0.34

T /K	w_1	w_2	Set A
333.15	0.050 ± 0.002	0.900 ± 0.003	4.86 ± 0.47
	0.900 ± 0.013	0.050 ± 0.010	14.25 ± 0.47
	0.300 ± 0.003	0.600 ± 0.003	6.03 ± 0.47
	0.600 ± 0.006	0.300 ± 0.006	9.33 ± 0.47
	0.100 ± 0.002	0.600 ± 0.002	2.57 ± 0.47

	0.300 ± 0.003	0.400 ± 0.003	3.51 ± 0.47
	0.600 ± 0.006	0.100 ± 0.006	5.75 ± 0.47
	0.250 ± 0.002	0.250 ± 0.002	1.92 ± 0.47

T /K	w_1	w_2	Set A
343.15	0.050 ± 0.002	0.900 ± 0.003	3.76 ± 0.46
	0.900 ± 0.013	0.050 ± 0.010	9.76 ± 0.46
	0.300 ± 0.003	0.600 ± 0.003	4.50 ± 0.46
	0.600 ± 0.006	0.300 ± 0.006	6.63 ± 0.46
	0.100 ± 0.002	0.600 ± 0.002	2.04 ± 0.46
	0.300 ± 0.003	0.400 ± 0.003	2.70 ± 0.46
	0.600 ± 0.006	0.100 ± 0.006	4.15 ± 0.46
	0.250 ± 0.002	0.250 ± 0.002	1.55 ± 0.46

T /K	w_1	w_2	Set A (1)	Set A (2)	Set C
353.15	0.050 ± 0.002	0.900 ± 0.003	2.96 ± 0.31	2.98 ± 0.31	-
	0.900 ± 0.013	0.050 ± 0.010	6.96 ± 0.31	6.96 ± 0.31	-
	0.300 ± 0.003	0.600 ± 0.003	3.47 ± 0.31	3.47 ± 0.31	3.47 ± 0.31
	0.600 ± 0.006	0.300 ± 0.006	4.89 ± 0.31	4.88 ± 0.31	-
	0.100 ± 0.002	0.600 ± 0.002	1.66 ± 0.31	1.66 ± 0.31	-
	0.300 ± 0.003	0.400 ± 0.003	2.12 ± 0.31	2.13 ± 0.31	-
	0.600 ± 0.006	0.100 ± 0.006	3.10 ± 0.31	3.13 ± 0.31	-
	0.250 ± 0.002	0.250 ± 0.002	1.25 ± 0.31	1.26 ± 0.31	1.26 ± 0.31

[a] Weight fractions and viscosities are reported with their expanded uncertainties (0.95 level of confidence). Expanded uncertainties not included above are $U(T) = 0.02$ K and $U(p) = 0.0030$ MPa.

As expected, viscosity increases as temperature decreases. Actually, a rather dramatic increase with temperature is observed especially for MDEA, exhibiting viscosity of 7.4 mPa·s at 353.15 K and viscosity of 198.1 mPa·s at 283.15 K. The variation of viscosity for MEG at the temperature limits of the study is far smaller than for MDEA. The same temperature effect is shown for the multicomponent systems, whose viscosity is also increasing with increasing amine concentration. The binary system MDEA-H_2O exhibits its maximum viscosity value for MDEA concentration approximately 95 wt.% and then decreases (See Supporting Information for a graphical presentation). Viscosity extremums (minimum, maximum or both) are not uncommon[60] and several authors have observed such behavior in amine-water systems[15,16,18,45,61]. The lower the temperature, the more pronounced the maximum in the viscosity curve is. This behavior is not followed for the MDEA-MEG or MEG-H_2O binary system, as indicated in **Figure 4** and **Figure S5**, which show the binary plots generated by comparing the fitted NRTL-DVIS model and real experimental data. The observed viscosity behavior can be explained by the theory of free-volumes which is further discussed in **Section 3.3**.

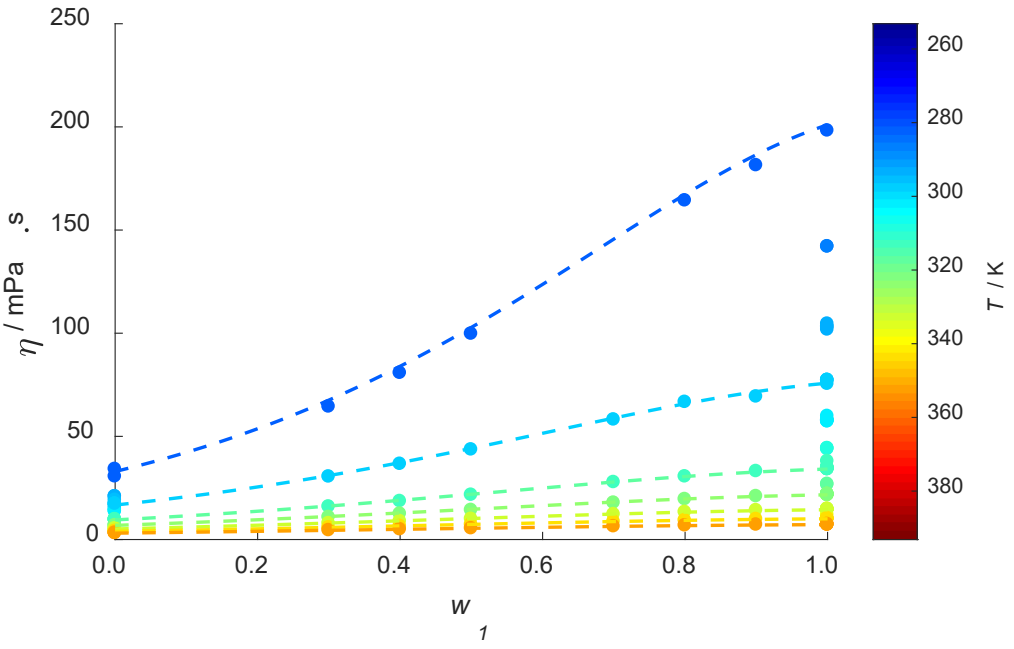

Figure 4. Binary data set of viscosities for {MDEA (1) + MEG (2)} and estimations generated by the NRTL-DVIS model. The temperature in which each experimental point (●) was measured is color-coded by the bar on the right side. The temperatures in which the estimates were made were 283.15 K (dark blue dashed line), 298.15 K (capri blue dashed line), 313.15 K (aqua dashed line), 323.15 K (green dashed line), 333.15 K (lime green dashed line), 343.15 K (yellow dashed line) and 353.15 K (orange dashed line).

According to the modeling procedure described in the previous section, the Vogel equation was employed for the estimation of the pure component viscosity. The results for the parametrization of the Vogel equation, presented in **Table 11**, show that the viscosities of the pure components are predicted with a satisfactory accuracy. Although the scatter observed for density data is not seen in the viscosity data, the huge variation of viscosity values with temperature (see **Figure 5**) generates AARDs worse than those observed for the fitting of density models. This variation with

360 temperature makes the fitting of viscosity models more difficult than that of density models, as
361 will be seen briefly.

362 **Table 11.** Parameters and results for the fittings of the Vogel equation

Parameter	MDEA	MEG
$\hat{A}$	-4.3997	-3.8670
$\hat{B}$	1302.2	1087.1
$\hat{C}$	148.94	135.50
$AARD$ (%)	1.10	2.47
MAD $(mPa \cdot s)$	3.76	2.46

363

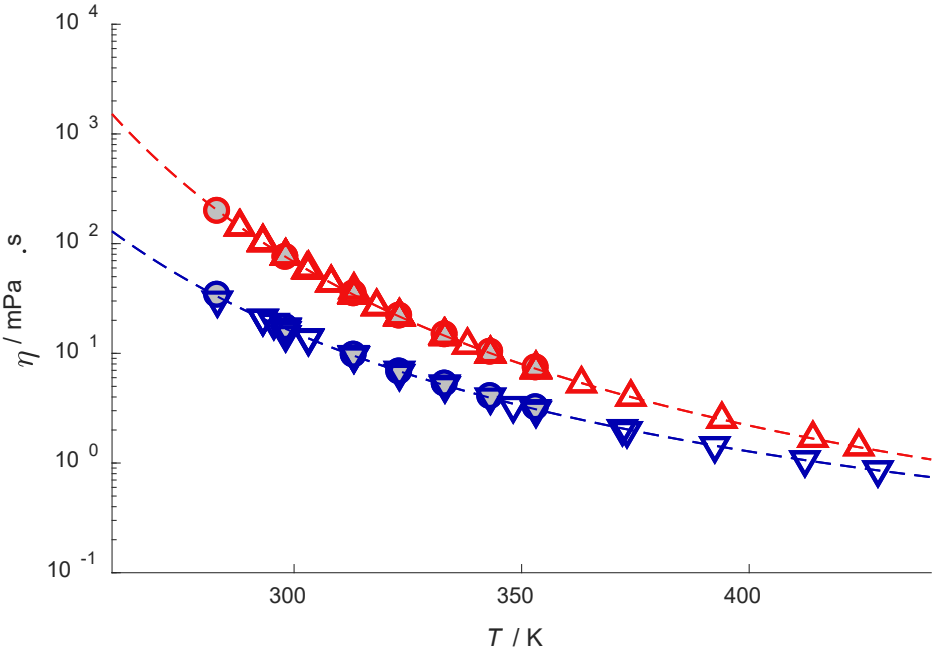

364

365 **Figure 5.** Experimental single component viscosity of MDEA both obtained in literature (red Δ)
366 as produced in this work (red ○ filled in grey) and of MEG both obtained in literature (blue ∇) as

produced in this work (blue ○ filled in grey), plus corresponding estimations with the Vogel equation for MDEA (red dashed line) and MEG (blue dashed line).

Both the Aspen liquid mixture viscosity model and the NRTL-DVIS were tested. One data point from our measurements for MDEA-MEG binary system was excluded as an outlier (T = 283.15 K, w_1 = 0.7). The data fitting parameters and results are shown in **Table 12** and **Table 13** for the Aspen model and the NRTL-DVIS respectively. Overall, the Aspen liquid mixture viscosity model showed a slightly worse performance than the NRTL-DVIS equation, returning AARD = 4.39% and MAD = 16.64 mPa·s whereas the latter showed AARD = 2.97% and MAD = 12.62 mPa·s. For the Aspen model, these deviations are more noticeable at lower temperature and viscosity ranges, though they are also present at higher temperatures and viscosities. The previously discussed maximum exhibited in the MDEA-H_2O system towards higher concentrations of MDEA is particularly problematic for the Aspen model to follow (see figures in Supporting Information). This difficulty in modeling strong non-ideal behavior also arises with the NRTL-DVIS equation, but to a much smaller extent. Comparison between the results of the NRTL-DVIS and the Aspen liquid viscosity model show that the fitting of the individual binaries returns higher or similar (for MEG-H_2O system) AARDs and MADs than the latter.

Table 12. Parameters and results for the Aspen liquid mixture viscosity model fitted for the global data set

Parameters of the Aspen liquid mixture viscosity model (1 = MDEA, 2 = MEG, 3 = water)					
$\hat{a}_{12}$	2.59783	$\hat{a}_{13}$	-1.37707	$\hat{a}_{23}$	0.02792
$\hat{b}_{12}$	-0.42333	$\hat{b}_{13}$	0.53470	$\hat{b}_{23}$	-0.16100

$\hat{c}_{12}$	2.74959	$\hat{c}_{13}$	-0.10402	$\hat{c}_{23}$	0.24937
$\hat{d}_{12}$	-0.98385	$\hat{d}_{13}$	-0.32799	$\hat{d}_{23}$	0.10408

Fitting results in terms of binary data sets					
MDEA-MEG		MDEA-water		MEG-water	
AARD (%)	2.41	AARD (%)	6.55	AARD (%)	2.22
MAD (mPa · s)	6.77	MAD (mPa · s)	16.64	MAD (mPa · s)	2.28

Fitting results in terms of the global data set	
AARD (%)	4.39
MAD (mPa · s)	16.64

385

386 **Table 13.** Parameters and results for the NRTL-DVIS equation fitted for the global data set

Parameters of the NRTL-DVIS model (1 = MDEA, 2 = MEG, 3 = water)					
$\hat{a}_{12}$	-0.75876	$\hat{a}_{13}$	-2.4116	$\hat{a}_{23}$	0.02129
$\hat{a}_{21}$	0.34081	$\hat{a}_{31}$	-0.81471	$\hat{a}_{32}$	5.4190
$\hat{b}_{12}$	442.83	$\hat{b}_{13}$	1710.7	$\hat{b}_{23}$	-46.130
$\hat{b}_{21}$	-244.71	$\hat{b}_{31}$	-180.36	$\hat{b}_{32}$	6636.7

α_{ij} = α = 0.3 ; R = 6.48803

Fitting results in terms of binary data sets					
MDEA-MEG		MDEA-water		MEG-water	
$AARD$ (%)	1.83	$AARD$ (%)	2.98	$AARD$ (%)	2.64
MAD $(mPa \cdot s)$	5.19	MAD $(mPa \cdot s)$	9.69	MAD $(mPa \cdot s)$	2.15
Fitting results in terms of the global data set					
$AARD$ (%)	2.97				
MAD $(mPa \cdot s)$	12.62				

387

388 In **Table 13**, one can notice that the largest deviation between estimated and experimental data
389 is obtained for the ternary system, which not only can show high viscosity variations but is also
390 subject to the non-idealities of mixing three very distinct components. The absolute relative
391 deviations (ARDs) between measured and estimated values for ternary systems can be observed
392 in Table S2 in the Supporting Information.

393 **Figure 6 (a)** and **(b)** show the parity plots between experimental and predicted viscosity data.
394 These figures show that the maximum deviations incurred by the NRTL-DVIS model are in the
395 order of 20 %, though the vast majority of it is within 10 %. The largest deviations are obtained
396 for the MDEA-water binary system (green *) and the MDEA-MEG-H_2O ternary system (purple
397 ◊). These are the conditions under which the widest span of viscosities is observed, which could

be the main reason for the fitting difficulties encountered. **Figure 6 (b)** suggests that there is no significant trend between the deviations and the temperature, whereas **Figure 6 (a)** shows that the model may underestimate the viscosities of binary MDEA-water systems and ternary systems at somewhat higher viscosities (noticed by the scatter of green * and purple ◊ above the zero line).

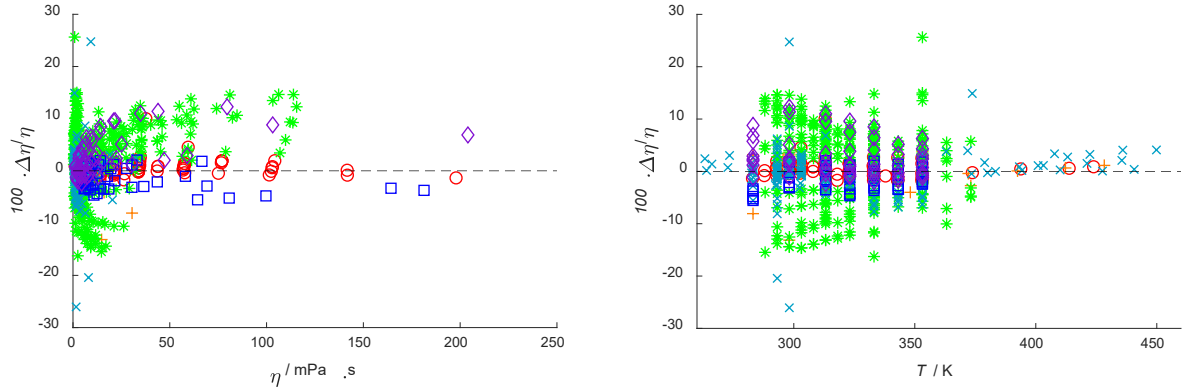

(a) (b)

Figure 6. Deviations in terms of differences between experimental and estimated viscosities divided by experimental viscosities regarding estimations made with the NRTL-DVIS model, and how they vary with the experimental viscosities themselves (a) and with temperature (b). The data sets are distributed in terms of pure MDEA data (red ○), pure MEG data (orange +), binary MDEA-water data (green *), binary MEG-water data (cyan ×), binary MDEA-MEG data (blue □) and ternary data (purple ◊).

3.3 Excess Properties

In order to further understand the molecular interactions of the system MDEA-MEG-H_2O, we calculated the excess molar volume v^E and viscosity deviations $\Delta\eta$ of the mixtures from the experimental results. For the calculation of excess molar volume v^E we used Eq. (4). The

calculated excess molar volumes and their uncertainties are shown in **Table 14** and **Figure 7** for MDEA-MEG and in **Table 15** for MDEA-MEG-H_2O.

Table 14. Excess molar volumes v^E / cm^3·mol^{-1} for {MDEA (1) + MEG (2)} as a Function of Weight Fraction w and Temperature T at Pressure p = 0.1020 MPa[a]

	v^E / cm^3·mol^{-1}			
w_1	T = 283.15 K	T = 298.15 K	T = 313.15 K	T = 323.15 K
0.000	0.000	0.000	0.000	0.000
0.300 ± 0.003	-0.267 ± 0.007	-0.247 ± 0.008	-0.255 ± 0.009	-0.268 ± 0.006
0.400 ± 0.003	-0.326 ± 0.008	-0.319 ± 0.008	-0.326 ± 0.008	-0.335 ± 0.006
0.500 ± 0.004	-0.367 ± 0.009	-0.357 ± 0.009	-0.363 ± 0.009	-0.374 ± 0.007
0.700 ± 0.006	-0.386 ± 0.012	-0.368 ± 0.11	-0.368 ± 0.011	-0.373 ± 0.010
0.800 ± 0.008	-0.336 ± 0.014	-0.307 ± 0.013	-0.307 ± 0.012	-0.306 ± 0.012
0.900 ± 0.009	-0.241 ± 0.018	-0.192 ± 0.018	-0.187 ± 0.017	-0.182 ± 0.017
1.000 ± 0.011	0.000	0.000	0.000	0.000

w_1	T = 333.15 K	T = 343.15 K	T = 353.15 K
0.000	0.000	0.000	0.000
0.300 ± 0.003	-0.246 ± 0.004	-0.237 ± 0.004	-0.230 ± 0.004
0.400 ± 0.003	-0.307 ± 0.004	-0.308 ± 0.004	-0.295 ± 0.004
0.500 ± 0.004	-0.351 ± 0.006	-0.341 ± 0.006	-0.328 ± 0.006
0.700 ± 0.006	-0.354 ± 0.009	-0.341 ± 0.009	-0.326 ± 0.009
0.800 ± 0.008	-0.293 ± 0.011	-0.281 ± 0.011	-0.264 ± 0.010
0.900 ± 0.009	-0.172 ± 0.016	-0.174 ± 0.016	-0.155 ± 0.017
1.000 ± 0.011	0.000	0.000	0.000

[a]Weight fractions and excess molar volumes are reported with their expanded uncertainties (0.95 level of confidence). Expanded uncertainties not included above are $U(T)$ = 0.02 K and $U(p)$ = 0.0030 MPa.

Table 15. Excess molar volumes v^E / cm^3·mol^{-1} for {MDEA (1) + MEG (2) + Water (3)} as a Function of Weight Fraction w and Temperature T at Pressure p = 0.1020 MPa[a]

		v^E / cm^3·mol^{-1}			
w_1	w_2	T = 283.15 K	T = 298.15 K	T = 313.15 K	T = 323.15 K
0.050 ± 0.002	0.900 ± 0.003	-0.210 ± 0.008	-0.181 ± 0.009	-0.179 ± 0.006	-0.211 ± 0.020
0.900 ± 0.013	0.050 ± 0.010	-0.707 ± 0.021	-0.670 ± 0.023	-0.657 ± 0.019	-0.674 ± 0.039
0.300 ± 0.003	0.600 ± 0.003	-0.571 ± 0.007	-0.533 ± 0.009	-0.514 ± 0.005	-0.533 ± 0.019
0.600 ± 0.006	0.300 ± 0.006	-0.856 ± 0.012	-0.815 ± 0.013	-0.792 ± 0.010	-0.801 ± 0.024
0.100 ± 0.002	0.600 ± 0.002	-0.508 ± 0.004	-0.455 ± 0.005	-0.421 ± 0.002	-0.407 ± 0.012
0.300 ± 0.003	0.400 ± 0.003	-0.724 ± 0.005	-0.666 ± 0.006	-0.633 ± 0.004	-0.613 ± 0.012
0.600 ± 0.006	0.100 ± 0.006	-1.089 ± 0.007	-1.026 ± 0.008	-0.985 ± 0.005	-0.969 ± 0.015
0.250 ± 0.002	0.250 ± 0.002	-0.570 ± 0.003	-0.512 ± 0.004	-0.489 ± 0.003	-0.466 ± 0.009

w_1	w_2	T = 333.15 K	T = 343.15 K	T = 353.15 K
0.050 ± 0.002	0.900 ± 0.003	-0.179 ± 0.024	-0.180 ± 0.024	-0.191 ± 0.032
0.900 ± 0.013	0.050 ± 0.010	-0.667 ± 0.046	-0.659 ± 0.045	-0.648 ± 0.059
0.300 ± 0.003	0.600 ± 0.003	-0.504 ± 0.022	-0.500 ± 0.022	-0.497 ± 0.029
0.600 ± 0.006	0.300 ± 0.006	-0.783 ± 0.028	-0.765 ± 0.027	-0.751 ± 0.036
0.100 ± 0.002	0.600 ± 0.002	-0.395 ± 0.014	-0.379 ± 0.014	-0.372 ± 0.018
0.300 ± 0.003	0.400 ± 0.003	-0.608 ± 0.015	-0.590 ± 0.014	-0.573 ± 0.019
0.600 ± 0.006	0.100 ± 0.006	-0.940 ± 0.018	-0.913 ± 0.018	-0.887 ± 0.024
0.250 ± 0.002	0.250 ± 0.002	-0.466 ± 0.011	-0.456 ± 0.011	-0.441 ± 0.014

[a]Weight fractions and excess molar volumes are reported with their expanded uncertainties (0.95 level of confidence). Expanded uncertainties not included above are $U(T)$ = 0.02 K and $U(p)$ = 0.0030 MPa.

For the binary system, excess molar volumes are negative in the whole range of compositions and temperatures studied in this work. Volume reduction upon mixing indicates the presence of charge-transfer and complex-forming interactions between MDEA and MEG, while it can also be the result of structural effects such as interstitial accommodation[62,63]. Both MDEA and MEG are polar molecules, therefore dipole-dipole interactions should be present between the partial negative charge of one molecule and the partial positive charge of another molecule. Additionally, autoprotolysis of MEG is reported in the literature[64,65] in the presence of MDEA, implying the breakage of the hydrogen bonding as a MEG molecule is losing its proton. In this case, dipole-ion forces between MDEA which acts as an electron donor and the cations formed from MEG autoprotolysis would appear. A minimum seems to occur between x_1= 0.4 and x_1= 0.5 (w_1=0.82 and w_2=0.87) indicating that these attractive intermolecular forces are strongest when the molar ratio between MDEA and MEG is close to 1:1.

As far as the temperature effect is concerned, **Figure 7** shows that the deviations from ideality become smaller when the temperature increases. This is expected and can be explained by the increase of the kinetic energy and weakening of the intermolecular forces at higher temperatures. In some cases, the calculated excess volume in different temperatures overlap. However, a closer look to the uncertainties listed in **Table 14** reveals that the observed overlaps lie within the uncertainty. Details about the uncertainty analysis of the excess molar volumes can be found in the Supporting Information.

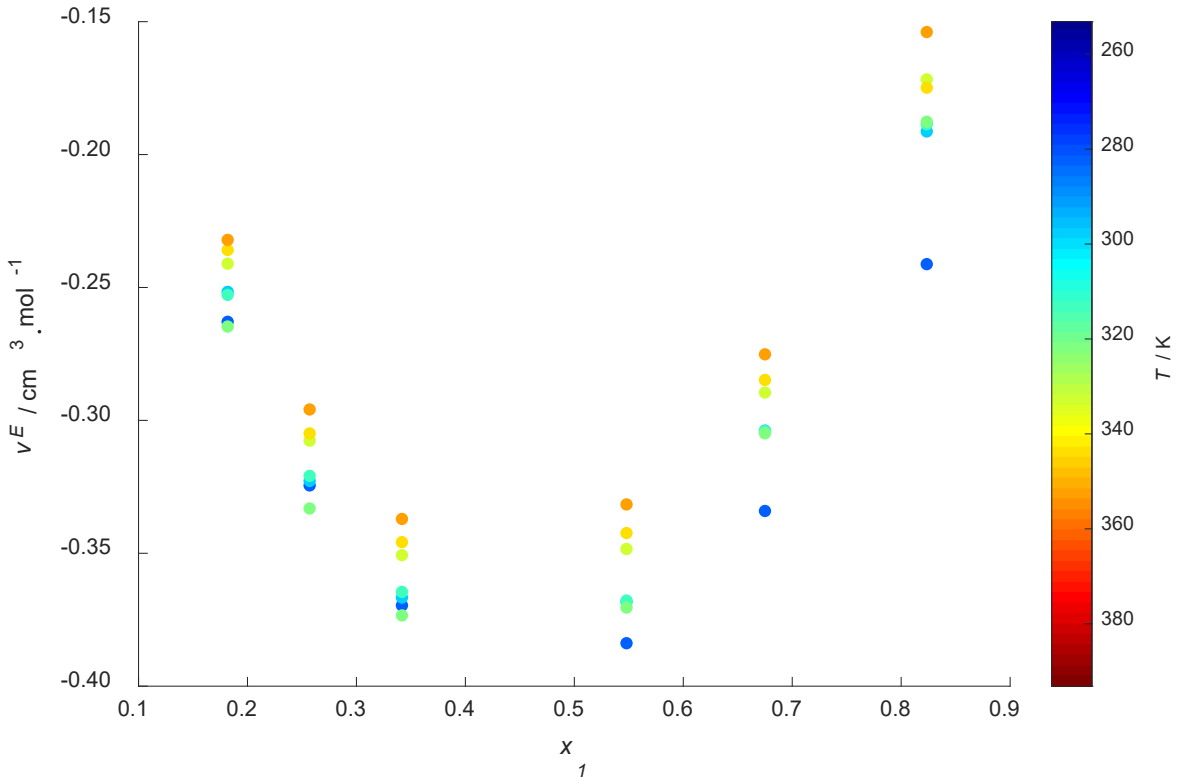

445

446 **Figure 7.** Excess molar volumes for {MDEA (1) + MEG (2)} as a function of molar fraction and
447 at temperatures 283.15 K (dark blue points), 298.15 K (capri blue points), 313.15 K (aqua points),
448 323.15 K (green points), 333.15 K (lime green points), 343.15 K (yellow points) and 353.15 K
449 (orange points).

450 The excess molar volumes for the ternary system are also negative, as one could speculate given
451 the negative deviations observed for the binary subsystems. Negative excess volumes have been
452 reported for MEG-H_2O by several researchers[23,25,26], with the exception of Yang et al.[24] who
453 reported positive v^E at T = (313.15 - 353.15) K and w_1 = 0.1 and 0.2. However, one would expect
454 that the miscibility of the mixture and the known affinity of MEG for water would lead to negative
455 excess molar volumes. As mentioned earlier, the excess volume is a contribution of both
456 intermolecular forces and structural effects. For the MEG-H_2O system, the dominating attractive

intermolecular forces due to the polarity of the molecules contribute to negative v^E. In addition, the structure of the water molecule has cavities due its hydrogen bonds, therefore it is expected that these empty spaces will be filled partially by other molecules, such as MEG and MDEA, leading also to negative excess volumes[61,66,67]. Negative deviations from ideality have been also reported for MDEA-H_2O system[10,14]. The MDEA protonation reaction with water is known in the literature[1] resulting in the formation of strong hydrogen bonds in the mixture. Therefore, higher compactness is expected for the MDEA-H_2O system in comparison with MEG-H_2O due to its strong hydrogen bonding. This is confirmed by the magnitude of their excess molar volumes; at 313.15 K for example, the minimum v^E is ca. -1.2 cm^3/mol for MDEA-H_2O and ca. -0.3 cm^3/mol for MEG-H_2O. The extreme minimum of -1.2 cm^3/mol appears at amine mole fraction close to x_1 = 0.3 (w_1 = 0.75) which is reflected in the previously mentioned maximum in density, observed at the same mole fraction for MDEA-H_2O mixtures. Therefore, the negative excess volumes for the ternary system would be the result of mainly the dipole-ion forces between MDEA and MEG, and hydrogen bonds between MDEA and water.

As mentioned under subsection *2.3 Computational Methods*, the viscosity deviations were calculated according to Eqs. (12)-(13). Calculation results and viscosity deviations' uncertainties are shown in **Table 16** and **Figure 8** for MDEA-MEG and in **Table 17** for MDEA-MEG-H_2O.

Table 16. Viscosity deviations $\Delta\eta$/mPa·s for {MDEA (1) + MEG (2)} as a Function of Weight Fraction w and Temperature T at Pressure p = 0.1020 MPa[a]

	$\Delta\eta$ / mPa·s			
w_1	T = 283.15 K	T = 298.15 K	T = 313.15 K	T = 323.15 K
0.000	0.00	0.00	0.00	0.00
0.300 ± 0.003	17.34 ± 4.01	7.82 ± 1.36	3.63 ± 0.82	2.36 ± 0.50
0.400 ± 0.003	27.03 ± 4.06	11.32 ± 1.37	5.02 ± 0.97	3.22 ± 0.50
0.500 ± 0.004	37.45 ± 5.09	14.97 ± 1.68	6.54 ± 0.83	4.04 ± 0.50
0.700 ± 0.006	-	19.30 ± 2.87	8.10 ± 0.91	4.80 ± 0.51
0.800 ± 0.008	52.26 ± 6.24	19.83 ± 3.02	7.38 ± 1.03	4.45 ± 0.54
0.900 ± 0.009	35.98 ± 8.99	11.06 ± 3.69	5.10 ± 1.13	3.04 ± 0.69
1.000 ± 0.011	0.00	0.00	0.00	0.00

w_1	T = 333.15 K	T = 343.15 K	T = 353.15 K
0.000	0.00	0.00	0.00
0.300 ± 0.003	1.44 ± 0.43	0.94 ± 0.64	0.69 ± 0.28
0.400 ± 0.003	1.93 ± 0.57	1.29 ± 0.64	0.91 ± 0.37
0.500 ± 0.004	2.42 ± 0.57	1.59 ± 0.63	1.09 ± 0.37
0.700 ± 0.006	2.86 ± 0.56	1.85 ± 0.61	1.24 ± 0.36
0.800 ± 0.008	2.65 ± 0.57	1.65 ± 0.61	1.11 ± 0.35
0.900 ± 0.009	1.71 ± 0.49	1.07 ± 0.64	0.74 ± 0.26
1.000 ± 0.011	0.00	0.00	0.00

[a]Weight fractions and viscosity deviations are reported with their expanded uncertainties (0.95 level of confidence). Expanded uncertainties not included above are $U(T)$ = 0.02 K and $U(p)$ = 0.0030 MPa.

Table 17. Viscosity deviations $\Delta\eta$ / mPa·s for {MDEA (1) + MEG (2) + Water (3} as a Function of Weight Fraction w and Temperature T at Pressure p = 0.1020 MPa[a]

		$\Delta\eta$ / mPa·s			
w_1	w_2	T = 283.15 K	T = 298.15 K	T = 313.15 K	T = 323.15 K
0.050 ± 0.002	0.900 ± 0.003	9.13 ± 2.75	4.50 ± 1.16	2.43 ± 1.10	1.73 ± 0.40
0.900 ± 0.013	0.050 ± 0.010	154.38 ± 6.08	57.22 ± 3.18	12.53 ± 2.10	13.63 ± 0.59
0.300 ± 0.003	0.600 ± 0.003	31.30 ± 3.11	14.00 ± 0.79	3.54 ± 1.06	4.62 ± 0.36
0.600 ± 0.006	0.300 ± 0.006	84.45 ± 4.11	34.27 ± 1.11	11.31 ± 1.07	9.53 ± 0.35
0.100 ± 0.002	0.600 ± 0.002	8.10 ± 2.44	4.29 ± 1.08	1.42 ± 1.04	1.82 ± 0.34
0.300 ± 0.003	0.400 ± 0.003	17.48 ± 2.44	8.57 ± 1.08	3.49 ± 1.04	3.21 ± 0.34
0.600 ± 0.006	0.100 ± 0.006	53.89 ± 2.44	22.20 ± 1.08	9.26 ± 1.04	6.69 ± 0.34
0.250 ± 0.002	0.250 ± 0.002	7.10 ± 2.44	3.63 ± 0.76	1.55 ± 1.04	1.50 ± 0.34

w_1	w_2	T = 333.15 K	T = 343.15 K	T = 353.15 K
0.050 ± 0.002	0.900 ± 0.003	1.15 ± 0.51	0.86 ± 0.53	0.65 ± 0.26
0.900 ± 0.013	0.050 ± 0.010	8.47 ± 0.57	5.49 ± 0.52	3.71 ± 0.26
0.300 ± 0.003	0.600 ± 0.003	3.17 ± 0.48	2.25 ± 0.48	1.66 ± 0.19
0.600 ± 0.006	0.300 ± 0.006	6.25 ± 0.48	4.24 ± 0.47	2.98 ± 0.22
0.100 ± 0.002	0.600 ± 0.002	1.34 ± 0.47	1.03 ± 0.46	0.81 ± 0.22
0.300 ± 0.003	0.400 ± 0.003	2.30 ± 0.47	1.71 ± 0.46	1.29 ± 0.22
0.600 ± 0.006	0.100 ± 0.006	4.59 ± 0.47	3.20 ± 0.46	2.32 ± 0.22
0.250 ± 0.002	0.250 ± 0.002	1.15 ± 0.47	0.90 ± 0.46	0.70 ± 0.18

[a]Weight fractions and viscosity deviations are reported with their expanded uncertainties (0.95 level of confidence). Expanded uncertainties not included above are $U(T)$ = 0.02 K and $U(p)$ = 0.0030 MPa.

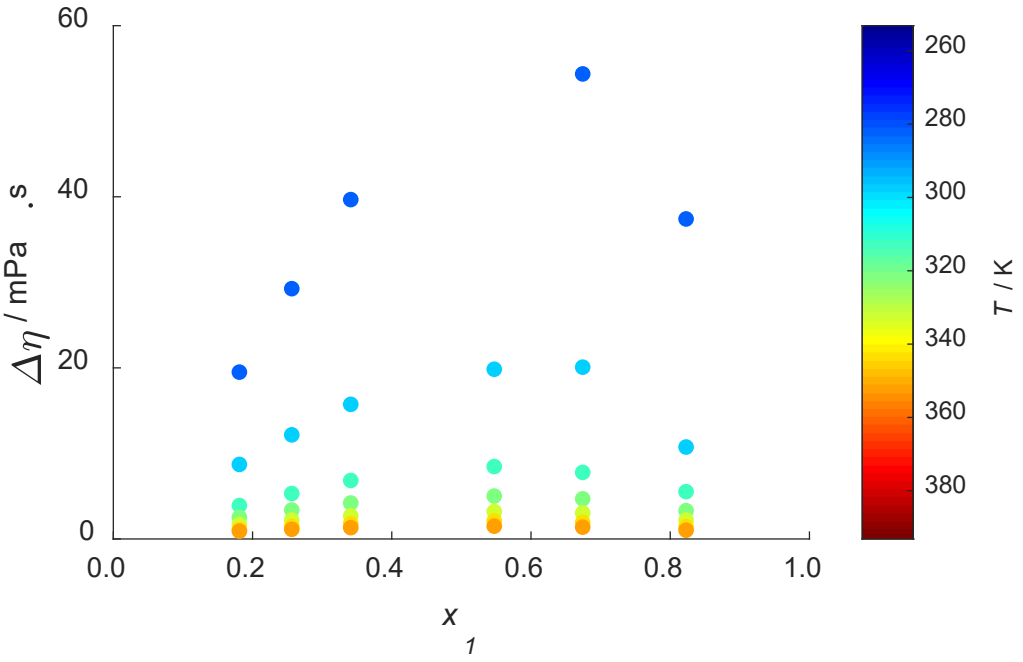

483

484 **Figure 8.** Viscosity deviations $\Delta\eta$ for {MDEA (1) + MEG (2)} as a function of molar fraction and
485 at temperatures 283.15 K (dark blue points), 298.15 K (capri blue points), 313.15 K (aqua points),
486 323.15 K (green points), 333.15 K (lime green points), 343.15 K (yellow points) and 353.15 K
487 (orange points).

488 The viscosity deviations for the binary systems MDEA-H_2O, MEG-H_2O, MDEA-MEG and the
489 ternary MDEA-MEG-H_2O are positive according to the literature and the additional findings of
490 this work. The positive viscosity deviations from ideality are expected based on the observed
491 negative molar volumes, which indicate the presence of strong molecular interactions between
492 these three chemical compounds, as discussed earlier. The strong hydrogen bonds in MDEA-H_2O
493 and dipole-ion forces in MDEA-MEG hinders the fluid to flow leading to viscosity increase with
494 MDEA concentration, as observed in **Figure S4** in Supporting Information and **Figure 4**
495 respectively. The former system exhibits viscosity increase with amine content up to
496 approximately 95 wt.% (x_1=0.75)[14]. It is possible that until this point, the attractive hydrogen bonds

predominate over the weaker molecule/ion-like forces. After this point, the abundance of amine or unavailability of water to protonate the amine could lead to greater contribution from the rest of the forces present in the system.

Temperature increase results in lower viscosity deviations due to the weakening of the intermolecular forces. Moreover, it is observed that, unlike in the case of excess volumes of MDEA-MEG where the minima were found at constant amine concentration between x_1=0.4 and x_1=0.5 for all temperatures studied in this work, the viscosity deviation maxima seem to appear around x_1=0.5 and shifting at higher mole fractions as the temperature decreases. In addition, there is a mismatch between the amine concentration at which the min v^E and max $\Delta\eta$ appear. This mismatch has been also observed for the binary MDEA-H_2O. According to Yin et al.[14] and Sathyanarayana et al.[68], this behavior can be explained by the effects based on the shape, size and structure of the molecules, which are able dominate over the intermolecular effects and even reverse the sign of the viscosity deviation.

The density and viscosity models developed in this work serve as an assessment tool for the successful employment of the binary MDEA-MEG or the ternary MDEA-MEG-H_2O systems at various temperature conditions. An example is the use of the developed viscosity model to construct viscosity contour plots, such as **Figure 9**, in order to identify the viscosity limits for operational reasons in a specific process. To read **Figure 9**, one can directly find the weight fraction of MEG in the X axis and the weight fraction of MDEA in the Y axis, so that the remainder of the mass will be denoted to water. In X = Y = 0, therefore, what is seen is the viscosity of pure water.

If one is concerned with avoiding a certain limiting viscosity when employing a MDEA-MEG-H_2O solution, for example 200 mPa·s at 278.15 K, **Figure 9** shows that systems with more than 80 wt.% MDEA approach or even exceed the viscosity specification and are not suitable. Alternatively, if one wants to find the viscosity of an 80 wt.% MDEA-15 wt.% MEG-5 wt.% H_2O, one should read 80 in the Y axis and 15 in the X axis, and find their viscosity at the point their imaginary lines intersect. At 288.15 K however, any composition for the ternary system respects the viscosity limit of 200 mPa·s.

In addition, similar to the observations made for the aqueous MDEA exhibiting maximum viscosity at approximately 95 wt.% MDEA, experimentally determined viscosities for the ternary system 90 wt.% MDEA - 5 wt.% MEG - 5 wt.% H_2O are also higher than the pure amine at temperatures lower than 313.15 K. Therefore, the addition of water as a means of reducing the viscosity for example in order to reach the viscosity specifications, should be used cautiously and after advising **Figure 9.** Naturally, knowing that the NRTL-DVIS model is underestimating the viscosities of MDEA-rich solutions, some additional attention should be paid. Overall, the models have been checked at temperatures outside the temperature range they were developed at, and it is observed that they are able to capture the trends for both density and viscosity. However, since the model is not validated outside the 283.15-353.15 K range as there are no experimental data available for the systems MDEA-MEG and MDEA-MEG-H_2O, any extrapolation must be performed with caution.

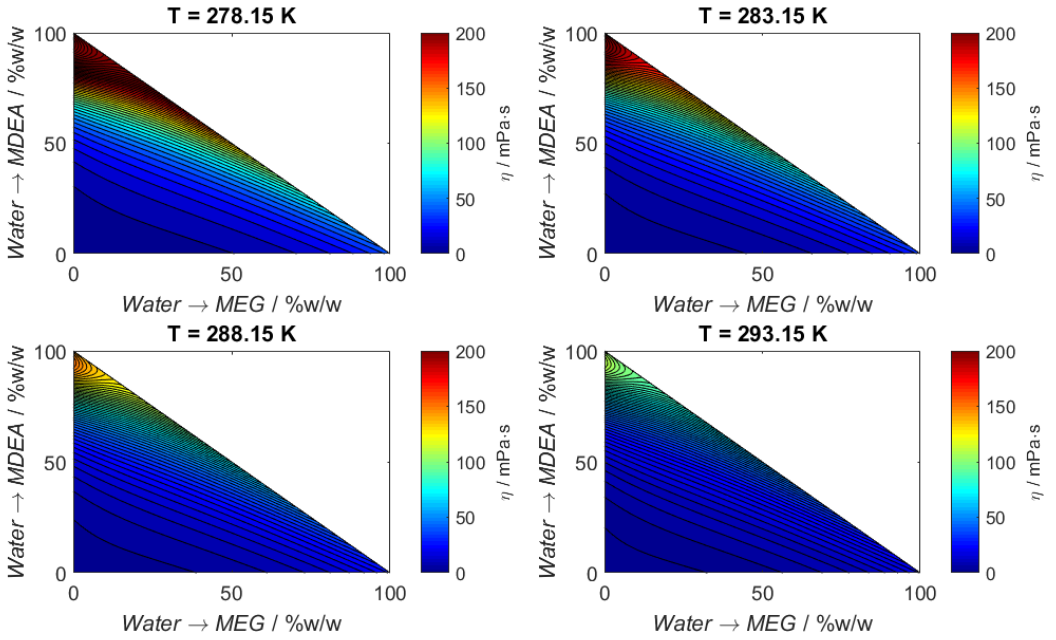

Figure 9. Viscosity plots for MDEA-MEG-water ternary mixtures in four different temperatures (278.15 K, 283.15 K, 288.15 K and 293.15 K). The viscosity values are color-coded by the bar on the right side.

4. CONCLUSIONS

New density and viscosity data were obtained for the systems MDEA-MEG and MDEA-MEG-H_2O at temperature T = (283.15 – 353.15) K, due to the potential application of the mixture for the combined H_2S removal and hydrate control in natural gas processing. The measurements showed good repeatability and reproducibility, while the excess molar volume and viscosity deviations upon mixing were calculated. Negative excess molar volumes and positive viscosity deviations indicated strong non-ideality of the mixtures at the studied compositions and temperatures. Density has been modeled successfully using NRTL-DVOL model, exhibiting AARD = 0.23%. The Aspen liquid mixture viscosity model and the NRTL-DVIS model were employed for the estimation of the viscosity data obtained in this work. They both perform satisfactorily, with the latter yielding

slightly better results. The results for the parametrization of the NRTL-DVIS model showed AARD = 2.97%.

NOMENCLATURE

Symbols	Unit	Meaning
a_{ij}, b_{ij}, c_{ij}, d_{ij}, G_{ij}, k_{ij}, l_{ij}, α_{ij}, τ_{ij}		Binary parameters for the density and viscosity models (DVOL, DVIS, Aspen liquid mixture viscosity model)
A_i, B_i, C_i		Single component parameters for the individual density and viscosity models (Rackett, Vogel)
MW_i	kg·mol	Molar weight of component i
NC		Number of components
NP		Number of points
p	Pa	Pressure
$p_{C,i}$	Pa	Critical pressure of component i
$p_{r,i}$		Reduced pressure of component i
R	$m^3 \cdot Pa \cdot K^{-1} \cdot mol^{-1}$	Ideal gas constant
T	K	Temperature
$T_{C,i}$	K	Critical temperature of component i
$T_{r,i}$		Reduced temperature of component i
v_i	$m^3 \cdot mol^{-1}$	Molar volume of component i
v^E	$m^3 \cdot mol^{-1}$	Excess molar volume of mixture
$Z_{RA,i}$		Compressibility factor of component i as obtained by the Rackett equation
w_i		Mass fraction of component i in a mixture
x_i		Molar fraction of component i in a mixture
Greek letters		
$\Delta\eta$	mPa·s	Viscosity deviation
η	mPa·s	Viscosity

η_i	mPa·s	Viscosity of single component i
$\hat{\eta}_{ij}$	mPa·s	Binary parameter for Aspen liquid mixture viscosity model
η^E	mPa·s	Excess viscosity
ρ	kg·m^{-3}	Density
ρ_i	kg·m^{-3}	Density of single component i
φ_{H2O}	P^{-1}	Water fluidity
Other notations		
Accent, e.g.: $\hat{y}$		Estimated variable, not measured
Bold, e.g.: $\boldsymbol{y}$		The variable is an array of variables

ASSOCIATED CONTENT

Supporting Information.

The Supporting Information file is available free of charge and it contains:

Experimental and predicted densities with NRTL-DVOL model
Experimental and predicted viscosities with NRTL-DVIS model
Experimental and predicted viscosities with Aspen liquid mixture viscosity model
Uncertainty Analysis

AUTHOR INFORMATION

Corresponding Author

*E-mail address: hanna.knuutila@ntnu.no

Author Contributions

The manuscript was written through contributions of all authors. All authors have given approval to the final version of the manuscript.

Funding Sources

This work was carried out as a part of SUBPRO (Subsea Production and Processing), a Research-based Innovation Centre within Subsea Production and Processing. The authors gratefully acknowledge the financial support from SUBPRO, which is financed by the Norwegian University of Science and Technology (NTNU), major industry partners and the Research Council of Norway (RCN) under project number 237893. The authors also acknowledge the financial support from the Faculty of Natural Sciences of NTNU.

REFERENCES

(1) Kohl, A. L.; Nielsen, R. B. *Gas Purification*, Fifth.; Gulf Professional Publishing: Houston, 1997.
(2) Campbell, J. M. Glycol Dehydration. In *Gas Conditioning and Processing*; Oklahoma, USA, 1998; Vol. 2, pp 333–394.
(3) Stewart, M.; Arnold, K. Part 2 - Gas Processing. In *Gas Sweetening and Processing Field Manual*; Arnold, M. S., Ed.; Gulf Professional Publishing: Boston, 2011; pp 141–155.
(4) Albuquerque, F. A.; Vianna, F. L. V.; Alves, R. P.; Kuchpil, C.; Morais, M. G. G.; Orlowski, R. T. C.; Moraes, C. A. C.; RIBEIRO, O. Subsea Processing Systems: Future Vision. In *OTC-24161-MS*; Offshore Technology Conference: OTC, 2013; p 14. https://doi.org/10.4043/24161-MS.
(5) Hutchinson, A. J. L. Process for Treating Gases. US2184596 A, October 24, 1939.
(6) McCartney, E. R. Gas Purification and Dehydration Process. US2435089 A, January 27, 1948.
(7) McCartney, E. R. Extraction of Acidic Impurities and Moisture from Gases. US2547278 A, April 3, 1951.
(8) Chapin, W. F. Purification and Dehydration of Gases. US2518752 A, August 15, 1950.
(9) Nookuea, W.; Tan, Y.; Li, H.; Thorin, E.; Yan, J. Impacts of Thermo-Physical Properties of Gas and Liquid Phases on Design of Absorber for CO2 Capture Using Monoethanolamine. *Int. J. Greenhouse Gas Control* **2016**, *52*, 190–200. https://doi.org/10.1016/j.ijggc.2016.07.012.
(10) Bernal-García, J. M.; Ramos-Estrada, M.; Iglesias-Silva, G. A.; Hall, K. R. Densities and Excess Molar Volumes of Aqueous Solutions of N-Methyldiethanolamine (MDEA) at Temperatures from (283.15 to 363.15) K. *J. Chem. Eng. Data* **2003**, *48* (6), 1442–1445. https://doi.org/10.1021/je030120x.
(11) Al-Ghawas, H. A.; Hagewiesche, D. P.; Ruiz-Ibanez, G.; Sandall, O. C. Physicochemical Properties Important for Carbon Dioxide Absorption in Aqueous Methyldiethanolamine. *J. Chem. Eng. Data* **1989**, *34* (4), 385–391. https://doi.org/10.1021/je00058a004.

(12) Li, M.-H.; Lie, Y.-C. Densities and Viscosities of Solutions of Monoethanolamine + N-Methyldiethanolamine + Water and Monoethanolamine + 2-Amino-2-Methyl-1-Propanol + Water. *J. Chem. Eng. Data* **1994**, *39* (3), 444–447. https://doi.org/10.1021/je00015a009.
(13) Paul, S.; Mandal, B. Density and Viscosity of Aqueous Solutions of (N-Methyldiethanolamine + Piperazine) and (2-Amino-2-Methyl-1-Propanol + Piperazine) from (288 to 333) K. *J. Chem. Eng. Data* **2006**, *51* (5), 1808–1810. https://doi.org/10.1021/je060195b.
(14) Yin, Y.; Fu, T.; Zhu, C.; Ma, Y. Volumetric and Viscometric Study and FT-IR Analysis of Binary and Ternary Mixtures of 1-Butyl-3-Methylimidazolium Tetrafluoroborate, Methyldiethanolamine and Water. *J. Mol. Liq.* **2017**, *243*, 664–676. https://doi.org/10.1016/j.molliq.2017.08.088.
(15) Teng, T. T.; Maham, Y.; Hepler, L. G.; Mather, A. E. Viscosity of Aqueous Solutions of N-Methyldiethanolamine and of Diethanolamine. *J. Chem. Eng. Data* **1994**, *39* (2), 290–293. https://doi.org/10.1021/je00014a021.
(16) Bernal-García, J. M.; Galicia-Luna, L. A.; Hall, K. R.; Ramos-Estrada, M.; Iglesias-Silva, G. A. Viscosities for Aqueous Solutions of N-Methyldiethanolamine from 313.15 to 363.15 K. *J. Chem. Eng. Data* **2004**, *49* (4), 864–866. https://doi.org/10.1021/je0302250.
(17) Pinto, D. D. D.; Johnsen, B.; Awais, M.; Svendsen, H. F.; Knuutila, H. K. Viscosity Measurements and Modeling of Loaded and Unloaded Aqueous Solutions of MDEA, DMEA, DEEA and MAPA. *Chem. Eng. Sci.* **2017**, *171*, 340–350. https://doi.org/10.1016/j.ces.2017.05.044.
(18) Chowdhury, F. I.; Akhtar, S.; Saleh, M. A. Viscosities and Excess Viscosities of Aqueous Solutions of Some Diethanolamines. *J. Mol. Liq.* **2010**, *155* (1), 1–7. https://doi.org/10.1016/j.molliq.2010.03.015.
(19) Rinker, E. B.; Oelschlager, D. W.; Colussi, A. T.; Henry, K. R.; Sandall, O. C. Viscosity, Density, and Surface Tension of Binary Mixtures of Water and N-Methyldiethanolamine and Water and Diethanolamine and Tertiary Mixtures of These Amines with Water over the Temperature Range 20-100.Degree.C. *J. Chem. Eng. Data* **1994**, *39* (2), 392–395. https://doi.org/10.1021/je00014a046.
(20) Baek, J.-I.; Yoon, J.-H.; Eum, H.-M. Physical and Thermodynamic Properties of Aqueous 2-Amino-2-Methyl-1,3-Propanediol Solutions. *Int. J. Thermophys.* **2000**, *21* (5), 1175–1184. https://doi.org/10.1023/A:1026454206200.
(21) Hayduk, Walter.; Malik, V. K. Density, Viscosity, and Carbon Dioxide Solubility and Diffusivity in Aqueous Ethylene Glycol Solutions. *J. Chem. Eng. Data* **1971**, *16* (2), 143–146. https://doi.org/10.1021/je60049a005.
(22) Bohne, D.; Fischer, S.; Obermeier, E. Thermal, Conductivity, Density, Viscosity, and Prandtl-Numbers of Ethylene Glycol-Water Mixtures. *Berichte der Bunsengesellschaft für physikalische Chemie* **1984**, *88* (8), 739–742. https://doi.org/10.1002/bbpc.19840880813.
(23) Sun, T.; Teja, A. S. Density, Viscosity, and Thermal Conductivity of Aqueous Ethylene, Diethylene, and Triethylene Glycol Mixtures between 290 K and 450 K. *J. Chem. Eng. Data* **2003**, *48* (1), 198–202. https://doi.org/10.1021/je025610o.
(24) Yang, C.; Ma, P.; Jing, F.; Tang, D. Excess Molar Volumes, Viscosities, and Heat Capacities for the Mixtures of Ethylene Glycol + Water from 273.15 K to 353.15 K. *J. Chem. Eng. Data* **2003**, *48* (4), 836–840. https://doi.org/10.1021/je020140j.

649 (25) Tsierkezos, N. G.; Molinou, I. E. Thermodynamic Properties of Water + Ethylene Glycol at
650 283.15, 293.15, 303.15, and 313.15 K. *J. Chem. Eng. Data* **1998**, *43* (6), 989–993.
651 https://doi.org/10.1021/je9800914.
652 (26) Afzal, W.; Mohammadi, A. H.; Richon, D. Volumetric Properties of Mono-, Di-, Tri-, and
653 Polyethylene Glycol Aqueous Solutions from (273.15 to 363.15) K: Experimental
654 Measurements and Correlations. *J. Chem. Eng. Data* **2009**, *54* (4), 1254–1261.
655 https://doi.org/10.1021/je800694a.
656 (27) Braun, N. O.; Persson, U. Å.; Karlsson, H. T. Densities and Viscosities of Mono(Ethylene
657 Glycol) + 2-Amino-2-Methyl-1-Propanol + Water. *J. Chem. Eng. Data* **2001**, *46* (4), 805–
658 808. https://doi.org/10.1021/je010004z.
659 (28) Song, J.-H.; Park, S.-B.; Yoon, J.-H.; Lee, H.; Lee, K.-H. Densities and Viscosities of
660 Monoethanolamine + Ethylene Glycol + Water. *J. Chem. Eng. Data* **1996**, *41* (5), 1152–
661 1154. https://doi.org/10.1021/je9601366.
662 (29) Li, L.; Zhang, J.; Li, Q.; Guo, B.; Zhao, T.; Sha, F. Density, Viscosity, Surface Tension, and
663 Spectroscopic Properties for Binary System of 1,2-Ethanediamine+diethylene Glycol.
664 *Thermochim. Acta* **2014**, *590*, 91–99. https://doi.org/10.1016/j.tca.2014.05.034.
665 (30) Zhao, T.; Zhang, J.; Li, L.; Guo, B.; Gao, L.; Wei, X. Excess Properties and Spectroscopic
666 Studies for the Binary System 1,2-Ethanediamine+polyethylene Glycol 300 at T=(293.15,
667 298.15, 303.15, 308.15, 313.15, and 318.15) K. *J. Mol. Liq.* **2014**, *198*, 21–29.
668 https://doi.org/10.1016/j.molliq.2014.07.004.
669 (31) DiGuilio, R. M.; Lee, R. J.; Schaeffer, S. T.; Brasher, L. L.; Teja, A. S. Densities and
670 Viscosities of the Ethanolamines. *J. Chem. Eng. Data* **1992**, *37*, 239–242.
671 (32) Álvarez, E.; Gómez-Díaz, D.; La Rubia, M. D.; Navaza, J. M. Densities and Viscosities of
672 Aqueous Ternary Mixtures of 2-(Methylamino)Ethanol and 2-(Ethylamino)Ethanol with
673 Diethanolamine, Triethanolamine, N-Methyldiethanolamine, or 2-Amino-1-Methyl-1-
674 Propanol from 298.15 to 323.15 K. *J. Chem. Eng. Data* **2006**, *51* (3), 955–962.
675 https://doi.org/10.1021/je050463q.
676 (33) Henni, A.; Maham, Y.; Tontiwachwuthikul, P.; Chakma, A.; Mather, A. E. Densities and
677 Viscosities for Binary Mixtures of N-Methyldiethanolamine plus Triethylene Glycol
678 Monomethyl Ether from 25 Degrees C to 70 Degrees C and N-Methyldiethanolamine plus
679 Ethanol Mixtures at 40 Degrees C. *J. Chem. Eng. Data* **2000**, *45* (2), 247–253.
680 https://doi.org/10.1021/je9902140.
681 (34) Haghtalab, A.; Shojaeian, A. Volumetric and Viscometric Behaviour of the Binary Systems
682 of N-Methyldiethanolamine and Diethanolamine with 1-Butyl-3-Methylimidazolium
683 Acetate at Various Temperatures. *J. Chem. Thermodyn.* **2014**, *68*, 128–137.
684 https://doi.org/10.1016/j.jct.2013.09.001.
685 (35) Akbar, M. M.; Murugesan, T. Thermophysical Properties for the Binary Mixtures of 1-
686 Hexyl-3-Methylimidazolium Bis(Trifluoromethylsulfonyl)Imide [Hmim][Tf2N]+N-
687 Methyldiethanolamine (MDEA) at Temperatures (303.15 to 323.15) K. *J. Mol. Liq.* **2012**,
688 *169*, 95–101. https://doi.org/10.1016/j.molliq.2012.02.014.
689 (36) Tsierkezos, N. G.; Molinou, I. E. Transport Properties of 2:2 Symmetrical Electrolytes in
690 (Water+ethylene Glycol) Binary Mixtures at T=293.15K. *J. Chem. Thermodyn.* **2006**, *38*
691 (11), 1422–1431. https://doi.org/10.1016/j.jct.2006.01.011.
692 (37) Jerome, F. S.; Tseng, J. T.; Fan, L. T. Viscosities of Aqueous Glycol Solutions. *J. Chem.*
693 *Eng. Data* **1968**, *13*, 496.

(38) Dunstan, A. E. IV.—The Viscosity of Liquid Mixtures. Part II. *J. Chem. Soc., Trans.* **1905**, *87* (0), 11–17. https://doi.org/10.1039/CT9058700011.
(39) Rumble, J. *CRC Handbook of Chemistry and Physics*; CRC press, 2017.
(40) Hartono, A.; Mba, E. O.; Svendsen, H. F. Physical Properties of Partially CO2 Loaded Aqueous Monoethanolamine (MEA). *J. Chem. Eng. Data* **2014**, *59* (6), 1808–1816. https://doi.org/10.1021/je401081e.
(41) Poli, R.; Kennedy, J.; Blackwell, T. Particle Swarm Optimization. *Swarm Intelligence* **2007**, *1* (1), 33–57. https://doi.org/10.1007/s11721-007-0002-0.
(42) Ghosh, S.; Das, S.; Kundu, D.; Suresh, K.; Abraham, A. Inter-Particle Communication and Search-Dynamics of Lbest Particle Swarm Optimizers: An Analysis. *Information Sciences* **2012**, *182* (1), 156–168. https://doi.org/10.1016/J.INS.2010.10.015.
(43) Pinto, D. D. D.; Svendsen, H. F. An Excess Gibbs Free Energy Based Model to Calculate Viscosity of Multicomponent Liquid Mixtures. *International Journal of Greenhouse Gas Control* **2015**, *42*, 494–501. https://doi.org/10.1016/J.IJGGC.2015.09.003.
(44) Evjen, S.; Wanderley, R.; Fiksdahl, A.; Knuutila, H. K. Viscosity, Density, and Volatility of Binary Mixtures of Imidazole, 2-Methylimidazole, 2,4,5-Trimethylimidazole, and 1,2,4,5-Tetramethylimidazole with Water. *Journal of Chemical & Engineering Data* **2019**, *64* (2), 507–516. https://doi.org/10.1021/acs.jced.8b00674.
(45) Pinto, D. D. D.; Monteiro, J. G. M.-S.; Johnsen, B.; Svendsen, H. F.; Knuutila, H. Density Measurements and Modelling of Loaded and Unloaded Aqueous Solutions of MDEA (N-Methyldiethanolamine), DMEA (N,N-Dimethylethanolamine), DEEA (Diethylethanolamine) and MAPA (N-Methyl-1,3-Diaminopropane). *International Journal of Greenhouse Gas Control* **2014**, *25*, 173–185. https://doi.org/10.1016/J.IJGGC.2014.04.017.
(46) Iloukhani, H.; Almasi, M. Densities and Excess Molar Volumes of Binary and Ternary Mixtures Containing Acetonitrile + Acetophenone + 1,2-Pentanediol: Experimental Data, Correlation and Prediction by PFP Theory and ERAS Model. *Journal of Solution Chemistry* **2011**, *40* (2), 284–298. https://doi.org/10.1007/s10953-010-9637-3.
(47) De Tucuman, S. M.; Acevedo, ; In& L L; Pedrosa, G. C.; Katz, M. *Excess Molar Volumes and Excess Viscosities of N-Butylamine + 1,4-Dioxane + Carbon Tetrachloride System at 298.15 K'*; 1990; Vol. 69.
(48) Cibulka, I. Estimation of Excess Volume and Density of Ternary Liquid Mixtures of Non-Electrolytes from Binary Data. *Collection of Czechoslovak Chemical Communications* **1982**, *47* (5), 1414–1419. https://doi.org/10.1135/cccc19821414.
(49) Nagata, I.; Tamura, K. Excess Molar Enthalpies for the Methanol-1-Butanol-Benzene System at 25.Degree.C. *Journal of Chemical & Engineering Data* **1988**, *33* (3), 283–285. https://doi.org/10.1021/je00053a018.
(50) Redlich, O.; Kister, A. T. Algebraic Representation of Thermodynamic Properties and the Classification of Solutions. *Industrial & Engineering Chemistry* **1948**, *40* (2), 345–348. https://doi.org/10.1021/ie50458a036.
(51) Singh, P. P.; Nigam, R. K.; Sharma, S. P.; Aggarwal, S. *Molar Excess Volumes of Ternary Mixtures of Nonelectrolytes*; 1984; Vol. 18.
(52) Pinto, D. D. D.; Knuutila, H. K. Density Calculations of Aqueous Amine Solutions Using an Excess Gibbs Based Model. *Braz. J. Chem. Eng.* **2019**.
(53) Arrhenius, S. Über Die Innere Reibung Verdünnter Wässeriger Lösungen. *Zeitschrift für Physikalische Chemie* **1887**, *1* (1), 285–298.

(54) Grunberg, L.; Nissan, A. H. Mixture Law for Viscosity. *Nature* **1949**, *164* (4175), 799–800. https://doi.org/10.1038/164799b0.
(55) Song, Y.; Mathias, P. M.; Tremblay, D.; Chen, C.-C. Liquid Viscosity Model for Polymer Solutions and Mixtures. *Industrial & Engineering Chemistry Research* **2003**, *42* (11), 2415–2422. https://doi.org/10.1021/IE030023X.
(56) Bingham, E. C.; Jackson, R. F. Standard Substances for the Calibration of Viscometers. *Journal of the Washington Academy of Sciences* **1917**, *7* (3), 53–55.
(57) Spieweck, F.; Bettin, H. Review: Solid and Liquid Density Determination / Übersicht: Bestimmung Der Dichte von Festkörpern Und Flüssigkeiten. *tm - Technisches Messen* **1992**, *59* (7–8), 285–292. https://doi.org/10.1524/teme.1992.59.78.285.
(58) Yaws, C. L. *Yaws' Critical Property Data for Chemical Engineers and Chemists*; Knovel: Norwich, NY, 2012.
(59) IAPWS R12-08: Viscosity of Ordinary Water http://www.iapws.org/relguide/viscosity.html (accessed Jun 7, 2019).
(60) Qunfang, L.; Yu-Chun, H. Correlation of Viscosity of Binary Liquid Mixtures. *Fluid Phase Equilibria* **1999**, *154* (1), 153–163. https://doi.org/10.1016/S0378-3812(98)00415-4.
(61) Hartono, A.; Svendsen, H. F. Density, Viscosity, and Excess Properties of Aqueous Solution of Diethylenetriamine (DETA). *The Journal of Chemical Thermodynamics* **2009**, *41* (9), 973–979. https://doi.org/10.1016/j.jct.2008.11.012.
(62) Iloukhani, H.; Almasi, M. Densities and Excess Molar Volumes of Binary and Ternary Mixtures Containing Acetonitrile + Acetophenone + 1,2-Pentanediol: Experimental Data, Correlation and Prediction by PFP Theory and ERAS Model. *J. Solution Chem.* **2011**, *40* (2), 284–298. https://doi.org/10.1007/s10953-010-9637-3.
(63) Rafiee, H. R.; Ranjbar, S.; Poursalman, F. Densities and Viscosities of Binary and Ternary Mixtures of Cyclohexanone, 1,4-Dioxane and Isooctane from T=(288.15 to 313.15)K. *The Journal of Chemical Thermodynamics* **2012**, *54*, 266–271. https://doi.org/10.1016/j.jct.2012.05.005.
(64) Eimer, D. *Gas Treating: Absorption Theory and Practice*; John Wiley & Sons, Inc: Chichester, West Sussex, 2014.
(65) Barzagli, F.; Lai, S.; Mani, F. Novel Non-Aqueous Amine Solvents for Reversible CO2 Capture. *Energy Procedia* **2014**, *63*, 1795–1804. https://doi.org/10.1016/j.egypro.2014.11.186.
(66) Wang, X.; Kang, K.; Wang, W.; Tian, Y. Volumetric Properties of Binary Mixtures of 3-(Methylamino)Propylamine with Water, N-Methyldiethanolamine, N,N-Dimethylethanolamine, and N,N-Diethylethanolamine from (283.15 to 363.15) K. *J. Chem. Eng. Data* **2013**, *58* (12), 3430–3439. https://doi.org/10.1021/je400679k.
(67) Maham, Y.; Teng, T. T.; Hepler, L. G.; Mather, A. E. Densities, Excess Molar Volumes, and Partial Molar Volumes for Binary Mixtures of Water with Monoethanolamine, Diethanolamine, and Triethanolamine from 25 to 80°C. *J Solution Chem* **1994**, *23* (2), 195–205. https://doi.org/10.1007/BF00973546.
(68) Sathyanarayana, B.; Ranjithkumar, B.; Savitha Jyostna, T.; Satyanarayana, N. Densities and Viscosities of Binary Liquid Mixtures of N-Methylacetamide with Some Chloroethanes and Chloroethenes at T=308.15K. *The Journal of Chemical Thermodynamics* **2007**, *39* (1), 16–21. https://doi.org/10.1016/j.jct.2006.06.009.

785 **For Table of Contents Only**

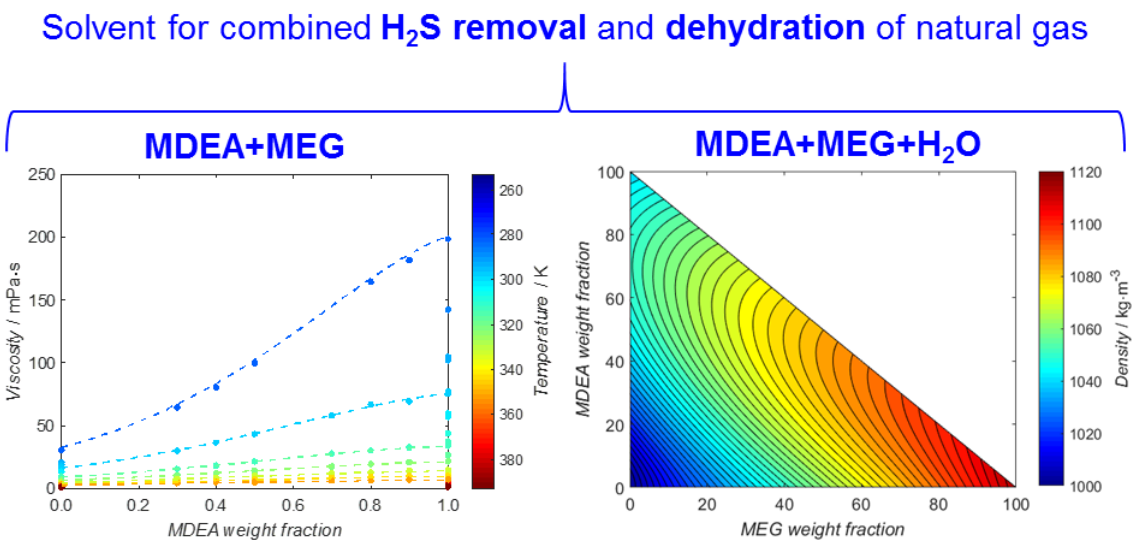

786